

Universality of large N phase transitions in Wilson loop operators in two and three dimensions

R. Narayanan

Department of Physics, Florida International University, Miami, FL 33199, USA
E-mail: rajamani.narayanan@fiu.edu

H. Neuberger

Rutgers University, Department of Physics and Astronomy, Piscataway, NJ 08855, USA
E-mail: neuberger@physics.rutgers.edu

ABSTRACT: The eigenvalue distribution of a Wilson loop operator of fixed shape undergoes a transition under scaling at infinite N . We derive a large N scaling function in a double scaling limit of the average characteristic polynomial associated with the Wilson loop operator in two dimensional QCD. We hypothesize that the transition in three and four dimensional large N QCD are also in the same universality class and provide a numerical test for our hypothesis in three dimensions.

KEYWORDS: $1/N$ Expansion, Lattice Gauge Field Theories.

Contents

1. Introduction.	2
2. Two dimensions: basics.	3
2.1 The average characteristic polynomial of the Wilson matrix.	4
2.1.1 Heat-kernel measure for W in the $SU(N)$ case.	4
2.1.2 $Q_N(z, t)$ does not self-average at finite N : $U(N)$ case.	5
2.1.3 Zeros of $Q_N(z, t)$ and the Lee-Yang theorem [6].	6
2.1.4 Derivation of the integral representation for $Q_N(z, t)$.	7
2.1.5 The average characteristic polynomial for negative areas.	11
2.2 The large N phase transition in $Q_N(z, t)$.	12
3. The double scaling limit.	13
3.1 General structure: dimensions 2, 3, 4.	13
3.1.1 Heuristic picture of the large N phase transition.	15
3.2 Structure in two dimensions.	16
4. Formulation of the large N universality hypothesis in dimensions 2,3,4.	17
4.1 Continuum formulation – ignoring renormalization.	18
4.1.1 Two dimensions: no renormalization needed.	18
4.2 Lattice formulation – completely defined.	19
4.2.1 Shape and scale of curves on the lattice.	19
4.2.2 Regularization of perimeter and corner divergences.	20
4.2.3 Universality hypothesis for square lattice Wilson loops.	21
4.2.4 Large N universality holds already before the continuum limit.	22
4.2.5 How to test for universal large N behavior numerically?	22
4.2.6 The estimates $b_c(L, N)$ for $b_c(L)$.	23
4.2.7 The estimates $a_2(L, N)$ for $a_2(L)$.	24
4.2.8 The estimates $a_1(L, N)$ for $a_1(L)$.	24
4.3 Example of a universality test on synthetic two dimensional data.	24
4.4 Volume dependence and large N reduction.	25
5. Three dimensions.	26
5.1 Details of the numerical analysis.	27
5.2 Extrapolation to infinite N .	28
5.3 Finite volume effects.	29
5.4 Extrapolation to infinite L – continuum extrapolation.	30
6. Summary and Discussion.	31

1. Introduction.

Intuitively, when the closed curve defining a Wilson loop operator is uniformly scaled we expect a qualitative change to occur: for small loops the parallel transport matrix round the loop is close to unity while for large loops this matrix should be as far from unity as possible, as a result of confinement. This is true in 2,3 and 4 Euclidean dimensions in pure YM, with gauge group $SU(N)$.

As the scale of the loop is varied, the operator goes from being sensitive to short distance physics to being sensitive to long distance physics. Somewhere on the way it undergoes a crossover. In a previous paper [1] we put forward the hypothesis that as N increases the crossover narrows and becomes a phase transition at infinite N , in the sense usually applied to individual large matrices. The eigenvalue distribution for small Wilson loops is centered around $+1$, and has a gap around -1 . The gap is eliminated for large loops and the eigenvalue distribution covers the entire circle, becoming uniform for asymptotically large loops. Confinement means that the uniform limit is approached with a correction that goes to zero exponentially in the square of the scale factor.

The hypothesis is more than just asserting a transition in the sense that the eigenvalue density has a point of non-analytic dependence on the scale parameter. The hypothesis also states that this phenomenon happens in 2, 3 and 4 Euclidean dimensions and that in all these dimensions the transitions are in the same universality class. For large N , close to the critical scale, all the complicated dependence on loop shape comes in only through a finite number of parameters, which are coefficients of terms dependent on sub-leading terms in N , of the form $N^{-\nu}$ with ν being universal exponents; further corrections in $\frac{1}{N}$ are less significant. The main exponent is related to the average eigenvalue spacing at -1 of the Wilson matrix close to criticality. The average spacing is then in between $\mathcal{O}(1)$, for a gap, and $\mathcal{O}(N^{-1})$, for nonzero eigenvalue density.

The purpose of this paper is to test our hypothesis in continuum YM in 3 Euclidean dimensions by numerical Monte Carlo simulation on the lattice. Critical behavior induced by taking an extensive parameter to infinity is often tested by numerically confirming the presumed universal approach to the respective thermodynamic limit. In the case of ordinary second order phase transitions one may seek to identify a finite-size scaling function. Something similar needs to be done in the case of large N transitions. The hypothesis we need to test says that the complicated 3 and 4 dimensional cases have the same universal behavior as the exactly solvable 2 dimensional case. In two dimensions we know much about the approach to infinite N , where the transition has been established long ago. We refer to this transition as the DO transition, after Durhuus and Olesen who discovered it [2]. Since we are using lattice methods to learn about continuum YM theory, we need to take the zero lattice spacing and infinite volume limits. We work under the assumption

that these limits interact simply with the large N limit. This is a standard assumption, and our results are consistent with it.

We first derive the universal behavior of a specific observable related to the Wilson matrix in two dimensions, where we work directly at infinite volume and in the continuum. We then take finite N “data” arrived at by employing exact analytical formulas and numerically check if this data exhibits the universal asymptotic behavior in the crossover. With these tools in hand we proceed to a numerical project in three dimensions, where in addition we need to handle statistical errors coming from the stochastic approximations used for the path integrals and systematic errors having to do with not working directly in the continuum and not at infinite volume. We exploit the relative ease to do simulations in three dimensions to make the statistical errors much smaller than absolutely necessary. Also, working at large N reduces finite volume effects, leaving the approach to continuum as the main new ingredient we need to get under control.

2. Two dimensions: basics.

The Wilson loop matrix in YM on the infinite plane is given by the product of many unitary matrices close to unity. Using methods first introduced by Migdal [3], the matrix associated with a curve that does not intersect itself is seen to be given by a product of a large number of independently and identically distributed (i.i.d.) unitary matrices. These unitary matrices are distributed in a small width around the unit matrix and the probability distribution of the Wilson loop matrix depends on a single parameter made out of the number of matrices and the width of their distribution. This parameter is in one to one correspondence to the area enclosed by the loop in units of the gauge coupling constant.

The multiplicative matrix model has been introduced by Janik and Wiczorek [4] who employed a solution method similar to that of Gopakumar and Gross [5]; we shall refer to it as the JW model. Its precise definition is: Let U_i with $i = 1, \dots, n$ be i.i.d. $N \times N$ unitary random matrices. $U_j = e^{i\epsilon H_j}$, where the hermitian matrix H_j is either unconstrained or traceless and distributed with a normalized probability density given by:

$$P(U_j) = \mathcal{N} e^{-\frac{N}{2} \text{Tr} H_j^2} \quad (2.1)$$

The parameter ϵ obeys $0 < \epsilon \ll 1$ and the integer n is large, so that the product $\epsilon^2 n$ is finite. We shall take the limit $n \rightarrow \infty$, $\epsilon \rightarrow 0$ with $t = n\epsilon^2$ kept fixed. t is related to the unit-less area mentioned above. The relation will be made precise later on. The Wilson loop matrix is given by:

$$W = \prod_{i=1}^n U_i \quad (2.2)$$

It turns out that the simplest gauge invariant observable made out of W which exhibits universal approach to critical behavior is the average characteristic polynomial of W , $\langle \det(z - W) \rangle$. The average characteristic polynomial is in one to one correspondence with the set of traces of W in all totally antisymmetric representations of $SU(N)$ or $U(N)$. Nontrivial representations with zero N -ality do not enter.

We shall derive integral and polynomial expressions for

$$Q_N(z, t) = \lim_{n \rightarrow \infty, \epsilon \rightarrow 0} \langle \det(z - W) \rangle |_{t=\epsilon^2 n} \text{ fixed} \quad (2.3)$$

that are valid for all N , separately for $SU(N)$ and for $U(N)$. These results are used to find the $N \rightarrow \infty$ limit, find a critical loop size in that limit, and then zoom into the the vicinity of this infinite N critical point. This vicinity is described by a “double scaling limit” of the average characteristic polynomial. The double scaling limit turns out to be identical for $SU(N)$ and for $U(N)$.

2.1 The average characteristic polynomial of the Wilson matrix.

We will derive the integral relation

$$Q_N(z, t) = \begin{cases} \sqrt{\frac{N\tau}{2\pi}} \int_{-\infty}^{\infty} d\nu e^{-\frac{N}{2}\tau\nu^2} \left[z - e^{-\tau\nu - \frac{\tau}{2}} \right]^N & \text{for } SU(N) \\ \sqrt{\frac{Nt}{2\pi}} \int_{-\infty}^{\infty} d\nu e^{-\frac{N}{2}t\nu^2} \left[z - e^{-t\nu - \frac{\tau}{2}} \right]^N & \text{for } U(N) \end{cases} \quad (2.4)$$

where $\tau = t(1 + \frac{1}{N})$. Given this relation, we can perform a binomial expansion and then compute the integral to obtain the polynomial relation

$$Q_N(z, t) = \begin{cases} \sum_{k=0}^N \binom{N}{k} z^{N-k} (-1)^k e^{-\frac{\tau k(N-k)}{2N}} & \text{for } SU(N) \\ \sum_{k=0}^N \binom{N}{k} z^{N-k} (-1)^k e^{-\frac{tk(N+1-k)}{2N}} & \text{for } U(N) \end{cases} \quad (2.5)$$

Before we proceed to give the details of the derivation of (2.4), we make some observations with regard to the polynomial expressions for $Q_N(z, t)$.

2.1.1 Heat-kernel measure for W in the $SU(N)$ case.

The definition of the $SU(N)$ random matrix ensemble produces an evolution in “time” of the probability distribution of the product matrix over the manifold of $SU(N)$. Invariance properties and locality imply that, up to some rescaling of the variable t to a variable τ , the probability distribution of the product matrix, W , will be given by the heat-kernel for $SU(N)$:

$$P(W, \tau) dW = \sum_R d_R \chi_R(W) e^{-\tau C_2(R)} dW \quad (2.6)$$

Here, dW is the Haar measure on $SU(N)$, R labels the irreducible representations of $SU(N)$, $C_2(R)$ is the second order Casimir in the representation R and $\chi_R(W)$ is the character of the representation R evaluated on the matrix W , with the convention that $\chi_R(\mathbf{1}) = d_R$ with d_R being the dimension of R . The normalization convention for the Casimir operator are related to the scale freedom in t . The normalization of the Haar measure dW is such that the characters $\chi_R(W)$ are orthonormal with respect to dW . Finally, the probability distribution is properly normalized such that $\int P(W, \tau) dW = 1$.

Let us now focus on the k -fold antisymmetric representations, $k = 1, \dots, N$ and label them by k . $C_2(k) = A_N \frac{k(N-k)}{2N}$ and $d_k = \binom{N}{k}$. We absorb A_N in the definition of τ . If the eigenvalues of W are $e^{i\theta_1}, e^{i\theta_2}, e^{i\theta_3}, \dots, e^{i\theta_N}$, and we define the moments, $M_k(t)$, by

$$M_k(t) = \left\langle \sum_{1 \leq j_1 < j_2 < j_3 \dots < j_k \leq N} e^{i(\theta_{j_1} + \theta_{j_2} + \dots + \theta_{j_k})} \right\rangle, \quad (2.7)$$

it follows that

$$M_k(t) = \langle \chi_k(W) \rangle = d_k e^{-\tau C_2(k)} = \binom{N}{k} e^{-\frac{\tau k(N-k)}{2N}} \quad (2.8)$$

Next we note that

$$Q_N(z, t) = \left\langle \prod_{j=1}^N (z - e^{i\theta_j}) \right\rangle = \sum_{k=0}^N z^{N-k} (-1)^k M_k(t) \quad (2.9)$$

and we are consistent with the $SU(N)$ case in (2.5) if we use (2.8) above. This consistency with a heat-kernel probability distribution for W provides a check of the derivation of (2.4) in the $SU(N)$ case.

2.1.2 $Q_N(z, t)$ does not self-average at finite N : $U(N)$ case.

The moments M_k defined in (2.7) are given by

$$M_k(t) = \begin{cases} e^{-\frac{\tau k(N-k)}{2N}} & \text{for } SU(N) \\ e^{-\frac{tk(N+1-k)}{2N}} & \text{for } U(N) \end{cases} \quad (2.10)$$

as seen by matching (2.9) with (2.5). We note that $M_k(t) = M_{N-k}(t)$ only for $SU(N)$ since W and W^\dagger are equally probable and $\det W = 1$.

There is insufficient information contained in the moments M to determine the joint probability distribution of the θ_i , or even of the average resolvent, $\langle \sum_{j=1}^N \frac{1}{z - e^{i\theta_j}} \rangle$. Nevertheless, $Q_N(z, t)$ is a polynomial in z and its zeros are determined by the coefficients M_k . Obviously, for any fixed W , the $e^{i\theta_j}$ are the zeros of $\det(z - W)$. Therefore, we expect the zeros of $Q_N(z, t)$ to represent in some manner the statistical properties of the $e^{i\theta_j}$. For any finite N there is no way to obtain the exact marginal distribution of even just a single eigenvalue of W (“one point function”) from the average characteristic polynomial. However, in the large N limit, this often becomes possible.

It is obvious that in our case, at finite N ,

$$\log \langle \det(z - W) \rangle \neq \langle \log \det(z - W) \rangle \quad (2.11)$$

for $U(N)$. This is seen already by comparing the z^0 term on the two sides. That $\langle \det W \rangle = M_N(t) = e^{-\frac{t}{2}}$ follows from (2.9) and (2.10). It is easy to understand the above result. The probability of any one of the hermitian matrices H_j factorizes into a factor depending only on the traceless part of H_j ($SU(N)$ part) and another depending just on $\text{Tr} H_j$ ($U(1)$ part): $\text{Tr} H^2 = \text{Tr}(H - \frac{1}{N} \text{Tr} H)^2 + \frac{1}{N} (\text{Tr} H)^2$. $\det W$ only depends on the $U(1)$ part and since this is the commuting part, we get

$$\langle \det(W) \rangle = e^{-\frac{n\epsilon^2}{2}} = e^{-\frac{t}{2}} \quad (2.12)$$

On the other hand, $\langle \log \det(W) \rangle = 0$.

Obviously, this example is specific to $U(N)$ and would not hold in the $SU(N)$ case. The observation is nevertheless useful as it provides an easy check of our derivation to follow. This might be viewed as a $\frac{1}{N}$ effect, since one would expect $\langle \det(W) \rangle \sim e^{-N(\dots)}$ at large N . This is consistent with the difference between $U(N)$ and $SU(N)$ being of lower order in $\frac{1}{N}$. However, since we are going to look at a more subtle large N limit, where we amplify a critical regime introducing extra dependences on N into some of the parameters z and t (a “double scaling” limit) we need to be careful about the distinction between $U(N)$ and $SU(N)$. Eventually we shall see that the difference between $U(N)$ and $SU(N)$ indeed does not matter as the exponents ν will be smaller than one. Thus, the universal corrections to the singular behavior at the critical point are larger than the $\frac{1}{N}$ correction differentiating $U(N)$ from $SU(N)$.

2.1.3 Zeros of $Q_N(z, t)$ and the Lee-Yang theorem [6].

We have commented already that the information about the true distribution of eigenvalues of the stochastic Wilson matrix is represented by the average characteristic polynomial only in a statistical sense, in that it would reproduce the moments contained in the coefficients of the characteristic polynomial, but not necessarily other spectral properties. We show now that the roots of the average characteristic polynomial in the case of $SU(N)$ are on the unit circle, similarly to the roots of every instance of the random Wilson matrix. This goes a long way toward justifying that the spectrum of the average characteristic polynomial itself can be seen as an approximation of the average spectrum of the Wilson loop matrix.

The polynomial expression for the $SU(N)$ in (2.5) is

$$Q_N(z, t) = (-1)^N e^{-\frac{N\tau}{8}} (-z)^{\frac{N}{2}} \sum_{k=0}^N \binom{N}{k} (-z)^{\frac{N}{2}-k} e^{\frac{\tau}{2N}(k-\frac{N}{2})^2} \quad (2.13)$$

Introduce now N Ising spins, $\sigma_i = \pm \frac{1}{2}$, $i = 1, \dots, N$ and the magnetization $M(\sigma) = \sum_{i=1}^N \sigma_i$. Then,

$$M(\sigma) = \frac{N}{2} - k \quad (2.14)$$

where k is the number of spins equal to $-\frac{1}{2}$ and varies between 0 and N .

Taking into account the number of configurations with k spins equal to $-\frac{1}{2}$ we get:

$$Q_N(z, t) = (-1)^N e^{-\frac{N\tau}{8}} (-z)^{\frac{N}{2}} \sum_{\sigma_1, \sigma_2, \dots, \sigma_N = \pm \frac{1}{2}} (-z)^{M(\sigma)} e^{\frac{\tau}{2N} M^2(\sigma)} \quad (2.15)$$

The self interaction terms from the magnetization squared can be extracted as a further prefactor. What remains is the partition function of an Ising model on an N vertex graph where every vertex is connected to every other vertex.

$$Z_N(z, t) = Q_N(z, t) (-1)^N e^{\frac{(N-1)\tau}{8}} (-z)^{-\frac{N}{2}} = \sum_{\sigma_1, \sigma_2, \dots, \sigma_N = \pm \frac{1}{2}} e^{\ln(-z) \sum_i \sigma_i} e^{\frac{\tau}{N} \sum_{i>j} \sigma_i \sigma_j} \quad (2.16)$$

The interaction is ferromagnetic for positive τ and there is a complex external magnetic field $\log(-z)$. The conditions of the Lee-Yang theorem [6] are therefore fulfilled and all roots of this partition function (and hence of the polynomial $Q_N(z, t)$) lie on the unit circle.

This is a result about the finite N average characteristic polynomial, which holds for all N in the $SU(N)$ case, but, as expected and explained earlier, cannot and does not hold in the $U(N)$ case, where the circle on which the eigenvalues lie shrinks exponentially with t .

2.1.4 Derivation of the integral representation for $Q_N(z, t)$.

We proceed to derive (2.4) through a series of statements. We will need the following external field integrals over H as part of our derivation. For $U(N)$ we have

$$\langle \langle e^{i\epsilon \text{tr}(HX)} \rangle \rangle = e^{-\frac{\epsilon^2}{2N} \text{tr}(X^2)} \quad (2.17)$$

and, for $SU(N)$ we have

$$\langle \langle e^{i\epsilon \text{tr}(HX)} \rangle \rangle = e^{-\frac{\epsilon^2}{2N} \text{tr}(X^2) + \frac{\epsilon^2}{2N^2} (\text{tr}(X))^2} \quad (2.18)$$

The $SU(N)$ formula gives $\langle \langle e^{i\epsilon \text{tr}(HX)} \rangle \rangle = 1$ for X proportional to the unit matrix, as expected, since $\text{tr}(HX) \propto \text{Tr}(H) = 0$.

An essential tool in our derivation is a path integral representation of the characteristic polynomial which is set up in the following statement.

Statement I:

$$\det(z - W) = \int \prod_{i=1}^n [d\psi_i d\bar{\psi}_i] e^{\sum_{i=1}^n [w\bar{\psi}_i \psi_i - \bar{\psi}_i U_i \psi_{i+1}]} \quad (2.19)$$

where $\bar{\psi}_i, \psi_i$ are Grassmann variables, $z = w^n$, $W = \prod_{i=1}^n U_i$ and $\psi_{n+1} = \psi_1$. As $n \rightarrow \infty$, $w \rightarrow 1$ while the complex variable $z = w^n$ is held fixed.

Proof: This statement reflects the obvious gauge invariance of the Grassmann system, in addition to a $Z(n)$ invariance under $w \rightarrow we^{\frac{2\pi i}{n}}$. The proof is by recursion. One step in the recursion process is

$$\int d\psi_j d\bar{\psi}_j e^{w\bar{\psi}_j \psi_j - \bar{\psi}_j U_j \psi_{j+1} - \bar{\psi}_n R_j \psi_j} = w^N e^{-\bar{\psi}_n R_{j+1} \psi_{j+1}} \quad (2.20)$$

with

$$R_{j+1} = \frac{1}{w} R_j U_j. \quad (2.21)$$

Noting that $R_1 = U_n$, we can repeat the single step above to integrate out all Grassmann variables except $\bar{\psi}_n$ and ψ_n and obtain the desired result of Statement I:

$$\begin{aligned} \int \prod_{i=1}^n [d\psi_i d\bar{\psi}_i] e^{\sum_{i=1}^n [w\bar{\psi}_i \psi_i - \bar{\psi}_i U_i \psi_{i+1}]} &= w^{N(n-1)} \int d\psi_n d\bar{\psi}_n e^{w\bar{\psi}_n \psi_n - \bar{\psi}_n R_n \psi_n} \\ &= w^{N(n-1)} \det(w - R_n) \\ &= \det(w^n - w^{n-1} R_n) \end{aligned}$$

$$= \det(z - W) \quad (2.22)$$

The derivation of (2.4) proceeds by first performing the average over U_j followed by the integration over the Grassmann variables. It will be useful to have an additional identity in the form of another Grassmann integral as stated below.

Statement II:

For $k > 1$,

$$\begin{aligned} e^{-\bar{\psi} Y^k \chi} &= \int \prod_{l=1}^{k-1} d\bar{\eta}_l^k d\eta_l^k e^{-\sum_{i=1}^{k-1} \bar{\eta}_i^k \eta_i^k - \bar{\psi} Y \eta_1^k + \sum_{i=1}^{k-2} \bar{\eta}_i^k Y \eta_{i+1}^k + \bar{\eta}_{k-1}^k Y \chi} \\ &\equiv \left\langle e^{-\bar{\psi} Y \eta_1^k + \sum_{i=1}^{k-2} \bar{\eta}_i^k Y \eta_{i+1}^k + \bar{\eta}_{k-1}^k Y \chi} \right\rangle_{\eta} \end{aligned} \quad (2.23)$$

Proof: For each $k > 1$, we have $(k-1)$ pairs of Grassmann variables denoted by $\bar{\eta}_l^k$ and η_l^k , $l = 1, \dots, (k-1)$. in the above statement. The proof of this statement also works by recursion. One step in the recursion process is

$$\int d\bar{\eta}_l^k d\eta_l^k e^{-\bar{\eta}_l^k \eta_l^k - \bar{\psi} Y^l \eta_l^k + \bar{\eta}_l^k Y \eta_{l+1}^k} = e^{-\bar{\psi} Y^{l+1} \eta_{l+1}^k} \quad (2.24)$$

Identifying $\eta_l^l = \chi$, we perform the above recursion $(k-1)$ times, starting from $l = 1$ to $l = (k-1)$ to obtain the result of Statement II.

We can use the result of the Statement II to perform the integral over U . We focus on one such integral in the following statement.

Statement III:

$$\left\langle e^{-\bar{\psi} U \chi} \right\rangle = e^{-\bar{\psi} \chi} \left\langle \left\{ \begin{array}{l} e^{-\frac{\epsilon^2}{2N} \text{Tr} X^2 + \frac{\epsilon^2}{2N^2} (\text{Tr} X)^2} \quad \text{for } SU(N) \\ e^{-\frac{\epsilon^2}{2N} \text{Tr} X^2} \quad \text{for } U(N) \end{array} \right\} \right\rangle_{\eta} \quad (2.25)$$

where the matrix X is

$$X_{ij} = \chi_i \bar{\psi}_j + \sum_{k=2}^{\infty} \frac{1}{(k!)^{1/k}} (\eta_1^k)_i \bar{\psi}_j - \sum_{k=3}^{\infty} \sum_{l=1}^{k-2} \frac{1}{(k!)^{1/k}} (\eta_{l+1}^k)_i (\bar{\eta}_l^k)_j - \sum_{k=2}^{\infty} \frac{1}{(k!)^{1/k}} \chi_i (\bar{\eta}_{k-1}^k)_j \quad (2.26)$$

Proof:

$$\begin{aligned} \left\langle e^{-\bar{\psi} U \chi} \right\rangle &= \left\langle e^{-\bar{\psi} e^{i\epsilon H} \chi} \right\rangle = \left\langle \prod_{k=0}^{\infty} e^{-\bar{\psi} \left[\frac{i\epsilon H}{(k!)^{1/k}} \right]^k \chi} \right\rangle \\ &= e^{-\bar{\psi} \chi} \int \prod_{k=2}^{\infty} \prod_{l=1}^{k-1} d\bar{\eta}_l^k d\eta_l^k e^{-\sum_{k=2}^{\infty} \sum_{l=0}^{k-1} \bar{\eta}_l^k \eta_l^k} \left\langle e^{-i\epsilon \text{Tr} H X} \right\rangle \\ &= e^{-\bar{\psi} \chi} \left\langle \left\{ \begin{array}{l} e^{-\frac{\epsilon^2}{2N} \text{Tr} X^2 + \frac{\epsilon^2}{2N^2} (\text{Tr} X)^2} \quad \text{for } SU(N) \\ e^{-\frac{\epsilon^2}{2N} \text{Tr} X^2} \quad \text{for } U(N) \end{array} \right\} \right\rangle_{\eta} \end{aligned} \quad (2.27)$$

We have used Statement II to obtain the third equality in (2.27) and we have used (2.17) and (2.18) to obtain the fourth equality in (2.27).

We can now perform the integrals over the full set of η and $\bar{\eta}$ variables to get the result of the following statement.

Statement IV

$$\langle e^{-\bar{\psi}U\chi} \rangle = \sqrt{\frac{N}{2\pi}} \int_{-\infty}^{\infty} d\lambda e^{-\frac{N}{2}\lambda^2} e^{-[1-\lambda\epsilon\sqrt{1+\frac{u}{N}}-\frac{1}{2}\epsilon^2(1-\frac{u}{N^2})] \bar{\psi}\chi} \quad (2.28)$$

with $u = 0$ for $U(N)$ and $u = 1$ for $SU(N)$.

Proof: In the limit of $n \rightarrow \infty$ and $\epsilon \rightarrow 0$, we can write

$$\left\langle e^{-\frac{\epsilon^2}{2N}\text{Tr}X^2 + \frac{\epsilon^2}{2N^2}(\text{Tr}X)^2} \right\rangle_{\eta} = e^{-\frac{\epsilon^2}{2N}\langle\text{Tr}X^2\rangle_{\eta} + \frac{\epsilon^2}{2N^2}\langle(\text{Tr}X)^2\rangle_{\eta}} \quad (2.29)$$

for $SU(N)$ and

$$\left\langle e^{-\frac{\epsilon^2}{2N}\text{Tr}X^2} \right\rangle_{\eta} = e^{-\frac{\epsilon^2}{2N}\langle\text{Tr}X^2\rangle_{\eta}} \quad (2.30)$$

for $U(N)$. The connected correlators of the exponent ignored above will result in terms of the form

$$F(\zeta) = \epsilon^2 f_1(\epsilon)\zeta + \epsilon \sum_{k=2}^{\infty} f_k(\epsilon)\zeta^k \quad (2.31)$$

where $\zeta = \epsilon\bar{\psi}\chi$ and $f_k(\epsilon)$, $k = 1, \dots, \infty$ have a power series expansion in ϵ with only non-negative powers. That the terms can only depend on the fermion bilinear $\bar{\psi}\chi$ is evident from symmetry arguments. Since X appears with one power of ϵ on the left hand side of (2.29) and (2.30), we can associate a $\sqrt{\epsilon}$ with each fermion. Every term in the connected correlator that contributes should have at least one term of the form $\bar{\eta}_l^k \eta_l^k$ that got integrated. This gives at least one extra power of ϵ . If the connected correlator has to result in ζ , the term should have at least two terms of the form $\bar{\eta}_l^k \eta_l^k$ since the relevant terms comes from $(\text{Tr}X^2)^2$, $(\text{Tr}X)^4$, $\text{Tr}X^2(\text{Tr}X)^2$ or higher powers of X . The extra powers of ϵ in (2.31) result in the vanishing of this term in the $\epsilon \rightarrow 0$ and $n \rightarrow \infty$ limit.

Even though X has an infinite number of terms, there are only two terms in $\langle\text{Tr}X^2\rangle_{\eta}$ and two terms in $\langle(\text{Tr}X)^2\rangle_{\eta}$:

$$\begin{aligned} \langle\text{Tr}X^2\rangle_{\eta} &= -(\bar{\psi}\chi)^2 - N\bar{\psi}\chi \\ \langle(\text{Tr}X)^2\rangle_{\eta} &= (\bar{\psi}\chi)^2 - \bar{\psi}\chi \end{aligned} \quad (2.32)$$

Inserting (2.32) into (2.29) and (2.30) and the result into Statement III gives us

$$\langle e^{-\bar{\psi}U\chi} \rangle = e^{-\bar{\psi}\chi} e^{\frac{\epsilon^2}{2N}(1+\frac{u}{N})(\bar{\psi}\chi)^2 + \frac{\epsilon^2}{2}(1-\frac{u}{N^2})\bar{\psi}\chi}, \quad (2.33)$$

with $u = 0$ for $U(N)$ and $u = 1$ for $SU(N)$.

Since,

$$\sqrt{\frac{N}{2\pi}} \int_{-\infty}^{\infty} d\lambda e^{-\frac{N}{2}\lambda^2 + \lambda\epsilon\sqrt{1+\frac{u}{N}}\bar{\psi}\chi} = e^{\frac{\epsilon^2}{2N}(1+\frac{u}{N})(\bar{\psi}\chi)^2} \quad (2.34)$$

the result in (2.33) reduces to statement IV.

Had we kept the term $F(\zeta)$ in (2.31), we can change the factor $e^{-\frac{N}{2}\lambda^2}$ in the integrand depending on the auxiliary fields λ to $e^{-\frac{N}{2}\lambda^2(1+P(\epsilon, \lambda))}$ so as to reproduce those terms. Alternatively, one can introduce an auxiliary field capturing the entire $F(\zeta)$ dependence using an inverse Laplace transform and interpreting it perturbatively (that is not worrying about the convergence of the λ integration, as anything beyond quadratic order is assumed to get expanded and truncated according to the power of ϵ). In either case one gets extra terms that will vanish in the correlated, large n – small ϵ , limit.

Now, we can use Statement IV to perform each U_i integral appearing in the expression for $\det(z - W)$ in Statement I resulting in the following statement.

Statement V

$$\begin{aligned} \langle \det(z - W) \rangle &= \left(\frac{N}{2\pi} \right)^{\frac{n}{2}} \int \prod_{i=1}^n d\lambda_i e^{-\frac{N}{2} \sum_{i=1}^n \lambda_i^2} \\ &\quad \int \prod_{i=1}^n [d\psi_i d\bar{\psi}_i] e^{\sum_{i=1}^n [w\bar{\psi}_i\psi_i - [1 - \lambda_i\epsilon\sqrt{1+\frac{u}{N}} - \frac{\epsilon^2}{2}(1-\frac{u}{N^2})]\bar{\psi}_i\psi_{i+1}]} \end{aligned} \quad (2.35)$$

We can now perform the Grassmann integrals exactly following the proof of Statement I for 1×1 matrices. The result is stated below.

Statement VI

$$\begin{aligned} \langle \det(z - W) \rangle &= \left(\frac{N}{2\pi} \right)^{\frac{n}{2}} \int \prod_{i=1}^n d\lambda_i e^{-\frac{N}{2} \sum_{i=1}^n \lambda_i^2} \\ &\quad \left[z - \prod_{i=1}^n \left[1 - \lambda_i\epsilon\sqrt{1+\frac{u}{N}} - \frac{\epsilon^2}{2} \left(1 - \frac{u}{N^2} \right) \right] \right]^N \end{aligned} \quad (2.36)$$

We are now set to proof the main result, namely, (2.4). We start by exponentiating the term inside the product of statement VI. One needs to take into account then a term of order $\epsilon^2\lambda_i^2$ which makes a finite contribution. This term is inserted into the exponentiated form in such a manner that the agreement between the exponentiated expression and the original one holds also at order ϵ^2 .

$$\begin{aligned} \langle \det(z - W) \rangle &= \left(\frac{N}{2\pi} \right)^{\frac{n}{2}} \int \prod_{i=1}^n d\lambda_i e^{-\frac{N}{2} \sum_{i=1}^n \lambda_i^2} \\ &\quad \left[z - e^{-\epsilon\sqrt{1+\frac{u}{N}} \sum_i \lambda_i - \frac{n\epsilon^2}{2} \left(1 - \frac{u}{N^2} \right) - \frac{\epsilon^2}{2} \left(1 + \frac{u}{N} \right) \sum_i \lambda_i^2} \right]^N \end{aligned} \quad (2.37)$$

Let $\Lambda = (\lambda_1, \lambda_2, \dots, \lambda_n)$. let r_1, r_2, \dots, r_n be an orthonormal basis with $r_1 = \frac{1}{\sqrt{n}}(1, \dots, 1)$. Finally, let $r_i \cdot \Lambda = \xi_i$. Then, using $t = n\epsilon^2$,

$$\langle \det(z - W) \rangle = \left(\frac{N}{2\pi} \right)^{\frac{n}{2}} \int \prod_{i=1}^n d\xi_i e^{-\frac{N}{2} \sum_{i=1}^n \xi_i^2} \left[z - e^{-\sqrt{t}\sqrt{1+\frac{u}{N}}\xi_1 - \frac{t}{2} \left(1 - \frac{u}{N^2} \right) - \frac{\epsilon^2}{2} \left(1 + \frac{u}{N} \right) \sum_i \xi_i^2} \right]^N \quad (2.38)$$

Now, let $\xi_1 = \sqrt{t}\mu$ and $\xi_k = \sqrt{n}\mu_k$ for $k = 2, \dots, n$. Then, again using $t = n\epsilon^2$,

$$\begin{aligned} \langle \det(z - W) \rangle &= \left(\frac{N}{2\pi} \right)^{\frac{n}{2}} \sqrt{tn}^{\frac{n-1}{2}} \int d\mu \int \prod_{i=2}^n d\mu_i e^{-\frac{N}{2}t\mu^2 - \frac{N}{2}n \sum_{i=2}^n \mu_i^2} \\ &\quad \left[z - e^{-t\sqrt{1+\frac{u}{N}}\mu - \frac{t}{2}\left(1-\frac{u}{N^2}\right) - \frac{t\epsilon^2}{2}\left(1+\frac{u}{N}\right)\mu^2 - \frac{t}{2}\left(1+\frac{u}{N}\right)\sum_{i=2}^n \mu_i^2} \right]^N \end{aligned} \quad (2.39)$$

Next, we go to polar coordinates in μ_i , $i = 2, \dots, n$ and set $r^2 = \sum_{i=2}^n \mu_i^2$. Then we get,

$$\begin{aligned} \langle \det(z - W) \rangle &= \left(\frac{N}{2\pi} \right)^{\frac{n}{2}} \sqrt{tn}^{\frac{n-1}{2}} \frac{2\pi^{\frac{n-1}{2}}}{\Gamma\left(\frac{n-1}{2}\right)} \int_{-\infty}^{\infty} d\mu \int_0^{\infty} dr r^{n-2} e^{-\frac{N}{2}t\mu^2 - \frac{N}{2}nr^2} \\ &\quad \left[z - e^{-t\sqrt{1+\frac{u}{N}}\mu - \frac{t}{2}\left(1-\frac{u}{N^2}\right) - \frac{t\epsilon^2}{2}\left(1+\frac{u}{N}\right)\mu^2 - \frac{t}{2}\left(1+\frac{u}{N}\right)r^2} \right]^N \end{aligned} \quad (2.40)$$

For large n , we can perform a saddle point calculation of the r integral. To leading order in n the saddle point is at $r_c = \sqrt{\frac{1}{N}}$ and we get

$$\begin{aligned} \langle \det(z - W) \rangle &= \left(\frac{N}{2\pi} \right)^{\frac{n}{2}} \sqrt{tn}^{\frac{n-1}{2}} \frac{2\pi^{\frac{n-1}{2}}}{\Gamma\left(\frac{n-1}{2}\right)} N^{-\frac{n}{2}} e^{-\frac{n}{2}} \sqrt{\frac{\pi}{nN}} N \int_{-\infty}^{\infty} d\mu e^{-\frac{N}{2}t\mu^2} \\ &\quad \left[z - e^{-t\sqrt{1+\frac{u}{N}}\mu - \frac{t}{2}\left(1+\frac{1}{N}\right) - \frac{t\epsilon^2}{2}\left(1+\frac{u}{N}\right)\mu^2} \right]^N \end{aligned} \quad (2.41)$$

Now we take the limit, $n \rightarrow \infty$, $\epsilon \rightarrow 0$ for a fixed t and we get

$$\langle \det(z - W(t)) \rangle = \sqrt{\frac{Nt}{2\pi}} \int_{-\infty}^{\infty} d\mu e^{-\frac{N}{2}t\mu^2} \left[z - e^{-t\sqrt{1+\frac{u}{N}}\mu - \frac{t}{2}\left(1+\frac{1}{N}\right)} \right]^N \quad (2.42)$$

Finally, we define $\tau = t\left(1 + \frac{1}{N}\right)$ and $\nu = \frac{\mu}{\sqrt{1+\frac{u}{N}}}$. Then the above equation reduces to (2.4).

We note that $U(N)$ and $SU(N)$ become indistinguishable in the large N double scaling limit we shall later employ. We will restrict ourselves to the $SU(N)$ case at finite N .

Since we are interested in the large N limit, we will not distinguish between τ and t and we will set

$$Q_N(z, t) = \sqrt{\frac{Nt}{2\pi}} \int_{-\infty}^{\infty} d\nu e^{-\frac{N}{2}t\nu^2} \left[z - e^{-t\left(\nu + \frac{1}{2}\right)} \right]^N \quad (2.43)$$

for all the discussion to follow. If we need to compare to continuum two dimensional YM, we should keep in mind that, on the basis of a comparison to a heat-kernel formula for the average characteristic polynomial, it is τ that is related directly to the inverse 't Hooft coupling, not t . In other words, there is a factor of $1 + \frac{1}{N}$ in the relationship between the parameter t of the JW model and the inverse 't Hooft coupling in the standard notation for the dimensionless area in two dimensional $SU(N)$ YM theory.

2.1.5 The average characteristic polynomial for negative areas.

The average characteristic polynomial depends on t in an analytic manner. In particular, it is interesting to consider the case $t \leq 0$. The conditions for applying the Lee-Yang theorem

no longer hold, as the interaction has become anti-ferromagnetic. Explicit examples show that all roots of the average characteristic polynomial are real and negative. On the other hand, it remains true for any t that if z is a root so are $\frac{1}{z}, z^*, \frac{1}{z^*}$. These symmetries are consistent with restricting all roots to the unit circle or to the positive or negative portions of the real axis. Thus, the symmetries alone do not tell much.

The case of $t \leq 0$ corresponds to imaginary ϵ , since $t = n\epsilon^2$. Imaginary ϵ corresponds to a complex Wilson matrix obtained by multiplying i.i.d. hermitian matrices close to identity. One would expect this Wilson matrix to have a spectrum covering a region of the complex plane in the stochastic sense. In this case we see that the roots of the average characteristic polynomial carry little information about the spectral properties of the Wilson matrix. This makes it clear why we carried out various checks to convince ourselves that the average characteristic polynomial was a useful observable for $t \geq 0$, when the matrices that get multiplied are unitary.

2.2 The large N phase transition in $Q_N(z, t)$.

We end up concluding that the average characteristic polynomial, $Q_N(z, t)$, at infinite N should reproduce the DO phase transition. In other words, one can replace the average of a logarithm by the logarithm of the average; this is somewhat analogous to a self averaging result proved by Berezin in 1972 [7].

We check that the DO transition is captured by the average characteristic polynomial by comparing our result to that of [4], who showed that the multiplicative matrix model has the DO phase transition using different methods, not involving the average characteristic polynomial, but rather accessing the resolvent $\lim_{N \rightarrow \infty} \frac{1}{N} \langle \text{tr} \frac{1}{z-W} \rangle$ directly. At infinite N , there is no distinction between $SU(N)$ and $U(N)$. We take the large N limit by finding the saddle point in μ that controls the integral; at the saddle point, $\nu = \lambda(t, z)$.

$$\frac{1}{N} \log Q_N(z, t) = -\frac{1}{2N} \log [1 + t(\lambda^2 + \lambda)] + \log \left(z - e^{-t(\lambda + \frac{1}{2})} \right) - \frac{t}{2} \lambda^2 \quad (2.44)$$

Here, λ solves:

$$\lambda = \lambda(t, z) = \frac{1}{ze^{t(\lambda + \frac{1}{2})} - 1} \quad (2.45)$$

To get the resolvent of W we take a derivative with respect to z . Only the explicit z dependence on the right hand side matters, since the expression is stationary with respect to variation in λ . We need to interchange the matrix averaging and the logarithm (a procedure we now have reason to believe will be valid in the limit of infinite N) at fixed t and z . The interchange can be viewed as a version of large N factorization, but now extended to a quantity that has an exponential dependence on N . This “self-averaging” property may also hold in the double scaling limit we shall introduce later, because violations of factorization would typically be (in view of the new type of observable) of order $\frac{1}{N}$ while the double scaling limit will be seen to add some dependencies in the couplings which are of slightly lower order coming in via factors of $\frac{1}{N^\nu}$ with $\nu = 1/2, 3/4$.

The expression for the resolvent in the large N limit is:

$$G = \frac{1}{N} \langle \text{Tr} \frac{1}{z - W} \rangle = \frac{1}{z - e^{-t(\lambda + \frac{1}{2})}} \quad (2.46)$$

JW define a function $f(t, z)$ by:

$$f(t, z) = zG(z, t) - 1 \quad (2.47)$$

and it is easy to see that f and λ are the same. The equation for λ can be rewritten as:

$$z\lambda = (1 + \lambda)e^{-t(\lambda + \frac{1}{2})} \quad (2.48)$$

leading to equation (17) in [4]. This allowed us to bypass the usage of the S -transform trick of [8] employed in [4]. We needed to bypass the usage of the S -transform trick, because we need the universal smoothed out behavior at asymptotically large, but not infinite, N , and the S -transform procedure has no known extension away from the infinite N limit.

We conclude that the average characteristic polynomial has a critical point at infinite N at $t = 4$, which is the location of the DO phase transition. The transition is reflected by the behavior around $z = -1$, which is where the gap in the eigenvalue is first opened.

3. The double scaling limit.

We wish to zoom into the region close to $z = -1$ when t is close to its critical value of 4. Our previous discussion has led us to conclude that a good quantity to look at is the derivative of the logarithm of the average characteristic polynomial with respect to z at $z = -1$. It simplifies matters to focus on the real z axis.

3.1 General structure: dimensions 2, 3, 4.

We set $z = e^y$ and define a function $F(y)$ from $Q_N(z, t)$ that is explicitly even in y :

$$F(y) = e^{-\frac{Ny}{2}} (-1)^N Q_N(-e^y, t) = \langle \det \left(e^{\frac{y}{2}} + e^{-\frac{y}{2}} W \right) \rangle \quad (3.1)$$

We have suppressed the dependence on t in the function $F(y)$.

We now introduce some new variables and notations:

$$\Upsilon = \tanh \frac{y}{2}, \quad A = \frac{1 - W}{1 + W} = -iM \quad (3.2)$$

A is anti hermitian and M is hermitian. If $e^{i\theta}$ is an eigenvalue of W , $-i \tan \frac{\theta}{2}$ is the corresponding eigenvalue of A and $\tan \frac{\theta}{2}$ of M . A, M become singular when the gap in the eigenvalue spectrum of W closes. The inverse transformation to W is:

$$W = \frac{1 - A}{1 + A} = \frac{1 + iM}{1 - iM}, \quad 1 + W = \frac{2}{1 + A} = \frac{2}{1 - iM} \quad (3.3)$$

The density of eigenvalues of W is denoted by $\rho_N(\theta)$, normalized by:

$$\int_{-\pi}^{\pi} \rho_N(\theta) \frac{d\theta}{2\pi} = N \quad (3.4)$$

$F(y)$ can be evaluated by Monte Carlo simulations in dimensions higher than 2.

$$F(y) = \left(2 \cosh \frac{y}{2} \right)^N \langle \det \left(\frac{1}{1+A} \right) \det(1 + \tanh \frac{y}{2} A) \rangle =$$

$$\left(\frac{4}{1-\Upsilon^2}\right)^{\frac{N}{2}} \langle \det\left(\frac{1}{1+A}\right) e^{-\sum_{n=1}^{\infty} (-1)^n \frac{\Upsilon^n}{n} \text{Tr} A^n} \rangle \quad (3.5)$$

This equation is still exact. For each A , $\det(1-A) = \det(1+A)$ on account of the $SU(N)$ condition $\det W = 1$. Since, in addition, the probability for an A equals that for a $-A$, $F(y)$ (which also depends on the loop and on the gauge coupling) is even in y (and, evidently then, in Υ). This can be made explicit:

$$F(y) = \left(\frac{4}{1-\Upsilon^2}\right)^{\frac{N}{2}} \langle \det\left(\frac{1}{1+A}\right) e^{-\sum_{k=1}^{\infty} \frac{\Upsilon^{2k}}{2k} \text{Tr} A^{2k}} \cosh\left(\sum_{k=1}^{\infty} \frac{\Upsilon^{2k-1}}{2k-1} \text{Tr} A^{2k-1}\right) \rangle \quad (3.6)$$

From the above equation one can derive exact expressions for the coefficients F_k in $F(y) = \sum_{k=0}^{\infty} F_k \Upsilon^{2k}$.

If the joint distribution of all the eigenvalues of A were known one could replace the averaging brackets on the right hand side by an integral over all eigenvalues weighted by that distribution. If we apply large N factorization, the right hand side simplifies considerably, and one is able to write it just in terms of the single eigenvalue distribution of A . From previous discussions we feel it is fine to assume that large N factorization holds in this case.

If we apply large N factorization, and use $\text{Tr} A^{2k+1} = 0$ for integer k , we obtain:

$$F_{\text{factorized}}(\Upsilon) = \left(\frac{4}{1-\Upsilon^2}\right)^{\frac{N}{2}} \frac{1}{\sqrt{\langle \det(1-A^2) \rangle}} \exp\left(-\sum_{k=1}^{\infty} \frac{\Upsilon^{2k}}{2k} \langle \text{Tr} A^{2k} \rangle\right) \quad (3.7)$$

In terms of M , we have:

$$F_{\text{factorized}}(\Upsilon) = \left(\frac{4}{1-\Upsilon^2}\right)^{\frac{N}{2}} \frac{1}{\sqrt{\langle \det(1+M^2) \rangle}} \exp\left(\sum_{k=1}^{\infty} (-1)^{k-1} \frac{\Upsilon^{2k}}{2k} \langle \text{Tr} M^{2k} \rangle\right) \quad (3.8)$$

Let the eigenvalues of M be denoted by λ . The eigenvalue density in θ , $\rho_N(2 \arctan y)$, which we now denote by an abuse of notation as $\rho_N(\lambda)$, is normalized by:

$$\frac{1}{\pi} \int \frac{d\lambda}{1+\lambda^2} \rho_N(\lambda) = N \quad (3.9)$$

$\rho_N(\lambda)$ is an even function: $\rho_N(\lambda) = \rho_N(-\lambda)$. When θ is close to $\pm\pi$, λ goes to $\pm\infty$. The critical regime around $\theta \approx \pm\pi$ we are interested in has been mapped to $\lambda \rightarrow \pm\infty$. The eigenvalue spacing in θ goes as the spacing in $\frac{1}{\lambda}$ in the large $|\lambda|$ regime.

Let us assume a very large, but finite N . If W is gap-less at infinite N at -1 , $\rho_N(\lambda) \sim cN$, $c > 0$ as $\lambda \rightarrow \pm\infty$. If W has a gap in the infinite N limit, $\rho_N(\lambda) \sim e^{-c'N}$, $c' > 0$ as $\lambda \rightarrow \pm\infty$. At the critical point when the gap just closes at $\pm\pi$, $\rho_N(\lambda) \sim c''N|\lambda|^{-\frac{1}{3}}$ [4], as $\lambda \rightarrow \pm\infty$.

If we now take the infinite N limit, $\frac{1}{N}\rho_N$ converges point-wise to a function ρ_{∞} that has compact support if there is a gap, infinite support with regular behavior at infinity if there is no gap and infinite support with a singular behavior at infinity if we are exactly at criticality. One can then re-express the logarithmic derivative of the factorized F

$$\frac{1}{N} \frac{\partial}{\partial \Upsilon} \log F_{\text{factorized}}(\Upsilon) = \frac{\Upsilon}{1-\Upsilon^2} + \frac{\Upsilon}{N} \langle \text{tr} \frac{M^2}{1+\Upsilon^2 M^2} \rangle = \frac{\Upsilon}{N(1-\Upsilon^2)} \langle \text{tr} \frac{1+M^2}{1+\Upsilon M^2} \rangle \quad (3.10)$$

in terms of $\rho_\infty(\lambda)$ as

$$\lim_{N \rightarrow \infty} \frac{1}{N} \frac{\partial}{\partial \Upsilon} \log F_{\text{factorized}}(\Upsilon) = \frac{1}{1 - \Upsilon^2} \frac{\Upsilon}{|\Upsilon|} \frac{1}{\pi} \int_{-\infty}^{\infty} d\lambda \frac{\rho_\infty\left(\frac{\lambda}{|\Upsilon|}\right)}{1 + \lambda^2} \quad (3.11)$$

3.1.1 Heuristic picture of the large N phase transition.

The determinant $\det(z - W)$ can be thought of as the exponent of a sum of N logarithms, one term for each eigenvalue. It is then the exponent of the two dimensional electrostatic potential created by N charges located at the zeros of the characteristic polynomial. These zeros are on the unit circle and we can look at the potential in the vicinity of the point -1 on this circle. There are two extreme cases: all charges are located at $+1$ or, the total charge is uniformly distributed on the circle.

For the extreme case where all charges are located at $+1$, $\rho_\infty(\lambda) = \pi\delta(\lambda)$. Inserting this into (3.11) results in

$$\frac{1}{N} \frac{\partial}{\partial \Upsilon} \log F_{\text{factorized}}(\Upsilon) = \frac{\Upsilon}{1 - \Upsilon^2} \quad (3.12)$$

For the other extreme case of a uniform distribution of charges on the unit circle, $\rho_\infty(\lambda) = 1$. Inserting this into (3.11) results in

$$\frac{1}{N} \frac{\partial}{\partial \Upsilon} \log F_{\text{factorized}}(\Upsilon) = \frac{\epsilon(\Upsilon)}{1 - \Upsilon^2} \quad (3.13)$$

Recalling that $\frac{\partial}{\partial \Upsilon} = \frac{2}{1 - \Upsilon^2} \frac{\partial}{\partial y}$ we conclude that

$$\frac{1}{N} \frac{\partial}{\partial y} \log F(y) = \begin{cases} \frac{1}{2} \tanh \frac{y}{2} & \text{for all charges at } +1 \\ \frac{1}{2} \epsilon(y) & \text{for uniform distribution of charges on the unit circle} \end{cases} \quad (3.14)$$

For a charge distribution that is critical, $\frac{1}{N} \frac{\partial}{\partial y} \log F(y)$ goes as $y^{\frac{1}{3}}$ as y goes to zero. If we now rescale the y variable by $N^{\frac{3}{4}}$, defining $y = \frac{\xi}{N^{\frac{3}{4}}}$, $\frac{1}{N} \frac{\partial}{\partial y} \log F(y)$ becomes of order $N^{-\frac{1}{4}}$ for fixed ξ .

The double scaling limit will smooth out the non-analyticity at $y = 0$ which we exhibited explicitly above for the case of a uniform distribution. At infinite N , there will always be a non-analyticity at $y = 0$ if the eigenvalue distribution has no gap, whether the distribution is uniform or not. The jump is proportional to the density of eigenvalues of W at $z = -1$, $\rho(\pi)$. On the other hand, when there is a gap, the behavior at $y = 0$ is smooth.

Up to a few non-universal parameters, the double-scaling limit captures the universal content of the non-analyticity. Neither of the two extreme limits that we have seen above, namely, a delta function and a uniform distribution, are necessary to be attainable in a particular model, for the transition represented by the non-analyticity we have seen to take place and be universally described by the scaling limit.

To match the scaling limit to the data of a particular physical realization, some parameters will need to be fit. For a large physical loop, one expects an almost uniform

distribution. Suppose now that we have a distribution that is almost uniform, with a small deviation from uniformity proportional to $\cos \theta$. In terms of λ ,

$$\rho(\lambda) = 1 + \delta \frac{1 - \lambda^2}{1 + \lambda^2} \quad (3.15)$$

Inserting this into (3.11) results in

$$\frac{1}{N} \frac{\partial}{\partial \Upsilon} \log F_{\text{factorized}}(\Upsilon) = \frac{\epsilon(\Upsilon)}{1 - v^2} \left[1 + \delta \frac{|\Upsilon| - 1}{|\Upsilon| + 1} \right] \quad (3.16)$$

In terms of the variable y , the result is

$$\frac{1}{N} \frac{\partial}{\partial y} \log F(y) = \frac{\epsilon(y)}{2} \left[1 - \delta e^{-|y|} \right] \quad (3.17)$$

For a large loop, when the deviation of the eigenvalue distribution from uniformity is small and determined by the string tension times the area t , we have $\delta \propto e^{-\sigma t}$. Positive and negative y values are related by a $Z(2)$ symmetry. The result is odd in y and undergoes a discontinuous change as y goes through 0. Taking a first derivative with respect to y of the above equation, we see that the area law term dominates for $y \neq 0$.

3.2 Structure in two dimensions.

Inserting (2.43) into the definition of $F(y)$ in (3.1) yields

$$F(y) = e^{-\frac{Ny}{2}} (-1)^N Q_N(-e^y, t) = 2^N e^{-\frac{Nt}{8}} \sqrt{\frac{Nt}{2\pi}} Z_N(y, t), \quad (3.18)$$

where,

$$Z_N(y, t) = \int dx e^{N[\log(\cosh \frac{y+tx}{2}) - \frac{1}{2}tx^2]} \quad (3.19)$$

We now extract from Z_N the same factor we had extracted from F :

$$Z_N(y, t) = \left(\cosh \frac{y}{2} \right)^N \int dx e^{N \left[\log \left(\frac{\cosh \frac{y+tx}{2}}{\cosh \frac{y}{2}} \right) - \frac{1}{2}tx^2 \right]} \quad (3.20)$$

Expanding the hyperbolic cosine of the sum in the exponent, we get:

$$Z_N(y, t) = \left(\cosh \frac{y}{2} \right)^N \int dx e^{N \left[\log(1 + \tanh \frac{y}{2} \tanh \frac{tx}{2}) - \frac{2}{t} \left(\frac{tx}{2} \right)^2 - \frac{1}{2} \log(1 - \tanh^2 \frac{tx}{2}) \right]} \quad (3.21)$$

We change variables of integration from x to $v = \tanh \frac{xt}{2}$. The inverse transformation is $\frac{xt}{2} = -\frac{1}{2} \log \frac{1-v}{1+v} = \sum_{k=0}^{\infty} \frac{v^{2k+1}}{2k+1}$.

$$Z_N(y, t) = \left(\cosh \frac{y}{2} \right)^N \frac{2}{t} \int_{-1}^1 \frac{dv}{1-v^2} e^{N \left[\log(1 + \tanh \frac{y}{2} v) - \frac{1}{2t} \left(\log \frac{1-v}{1+v} \right)^2 - \frac{1}{2} \log(1-v^2) \right]} \quad (3.22)$$

From now on, the integration over v will be implicitly understood to run from -1 to $+1$. We also introduce the parameter $\Upsilon = \tanh \frac{y}{2}$ with the understanding that Υ is real and that $|\Upsilon| \leq 1$. Expanding the exponent in v we have

$$\begin{aligned} Z_N(y, t) &= \left(\frac{1}{1 - \Upsilon^2} \right)^{\frac{N}{2}} \frac{2}{t} \int \frac{dv}{1 - v^2} \times \\ &\quad e^{N \left[\sum_{n=1}^{\infty} (-1)^{n-1} \frac{1}{n} \Upsilon^n v^n - \frac{2}{t} v^2 \left(\sum_{k=0}^{\infty} \frac{1}{2k+1} v^{2k} \right)^2 + \frac{v^2}{2} \left(\sum_{k=0}^{\infty} \frac{1}{k+1} v^{2k} \right) \right]} \\ &= \left(\frac{1}{1 - \Upsilon^2} \right)^{\frac{N}{2}} \frac{2}{t} \int \frac{dv}{1 - v^2} \times \\ &\quad e^{N \left[((\Upsilon v) - \frac{1}{2}(\Upsilon v)^2 + \frac{1}{3}(\Upsilon v)^3 + \dots) + \left((\frac{1}{2} - \frac{2}{t})v^2 + \frac{1}{4}v^4 - \frac{4}{3}\frac{v^4}{t} \dots \right) \right]} \end{aligned} \quad (3.23)$$

The critical point is at $t = 4$, where the coefficient of the term Nv^2 vanishes (the term of order v^2 that has a coefficient of order 1 does not matter, as we are interested in the large N critical point). The double scaling limit is defined so that the highest power of v (without a factor of Υ) is 4. This means that the integration variable v will be conveniently redefined as

$$v = \left(\frac{12}{N} \right)^{\frac{1}{4}} u \quad (3.24)$$

To keep a Υ dependence we need rescale Υ so that the variable ξ below is kept fixed as $N \rightarrow \infty$.

$$\Upsilon = \frac{\xi}{12^{\frac{1}{4}} N^{\frac{3}{4}}} \quad (3.25)$$

To keep the v^2 dependence we need to keep t close to 4, writing

$$\frac{4}{t} = 1 + \frac{\alpha}{\sqrt{3N}} \quad (3.26)$$

We end up with:

$$\lim_{N \rightarrow \infty} \left(\frac{4N}{3} \right)^{\frac{1}{4}} Z_N(y, t) = \int_{-\infty}^{\infty} du e^{-u^4 - \alpha u^2 + \xi u} \equiv \zeta(\xi, \alpha) \quad (3.27)$$

The above equation explicitly shows that keeping ξ and α fixed, while taking N to infinity will make the function $\left(\frac{4N}{3} \right)^{\frac{1}{4}} Z_N(y, t)$ converge point-wise to the α - and ζ - dependent limit given by $\zeta(\xi, \alpha)$. Looking at equation (3.23), we see that corrections will go as powers of $\frac{1}{\sqrt{N}}$. A plot of the logarithmic derivative of ζ with respect to ξ in Figure 1. shows that the double scaling limit provides a smoothed version for the non-analyticity discussed in (3.1.1).

4. Formulation of the large N universality hypothesis in dimensions 2,3,4.

We now abstract from the two dimensional case a hypothesis expected to hold also for Euclidean $SU(N)$ gauge theory in dimensions 3 and 4. We first formulate the statement in continuum ignoring renormalization, and next provide a precise formulation using lattice gauge theory as a constructive definition of continuum YM.

4.1 Continuum formulation – ignoring renormalization.

Suppose we have a Wilson loop associated with a curve \mathcal{C} , $W(\mathcal{C})$. Suppose the loop \mathcal{C} , is parametrically described by a closed, non-self-intersecting curve $x_\mu(s), s \in [0, 1]$. This description is redundant under re-parameterizations of the curve. Consider this curve together with an infinite family of scaled versions of it: $\mathcal{C}(m)$, described parametrically by $x_\mu(s, m) = \frac{1}{m}x_\mu(s)$, with $m > 0$. If we collect all these families we obtain the space of all loops. We wish to think about a single loop $\mathcal{C}(m)$ as being labeled by its shape $\mathcal{C}(*)$, which is the label of its scaled family and is described by dimensionless parameters, and a particular scale m which identifies it uniquely within the family and is of dimension mass. We now pick a loop shape and look at the family of operators $W(m, \mathcal{C}(*)) = W(\mathcal{C}(m))$. We are interested in the behavior of $W(m, \mathcal{C}(*))$ as we vary m , keeping $\mathcal{C}(*)$ fixed. More specifically, we are looking at

$$O_N(y, m, \mathcal{C}(*)) = \langle \det(e^{\frac{y}{2}} + e^{-\frac{y}{2}} W(m, \mathcal{C}(**))) \rangle \quad (4.1)$$

with particular interest focused on the region where y is close to 0.

The first part of the hypothesis is that the definition makes sense, meaning that $O_N(y, m, \mathcal{C}(**))$ is well defined, and that indeed there exists some scale m_c of the basic loop shape $\mathcal{C}(**)$ at which the Wilson matrix undergoes the DO large N phase transition. The part of the hypothesis that has to do with large N universality says that there exists a (non-universal) normalization $\mathcal{N}(N, m, \mathcal{C}(**))$, dependent on N , m and the loop shape, and finite dimensionless parameters $a_1(\mathcal{C}(**)), a_2(\mathcal{C}(**))$ such that

$$\lim_{N \rightarrow \infty} \mathcal{N}(N, b, \mathcal{C}(**)) O_N \left(y = \left(\frac{4}{3N^3} \right)^{\frac{1}{4}} \frac{\xi}{a_1(\mathcal{C}(**))}, m = m_c \left[1 + \frac{\alpha}{\sqrt{3N} a_2(\mathcal{C}(**))} \right] \right) = \zeta(\xi, \alpha) \quad (4.2)$$

4.1.1 Two dimensions: no renormalization needed.

In two dimensions, for a non-self-intersecting loop, the dependence on \mathcal{C} comes only through its total enclosed area; there is no dependence on $\mathcal{C}(**)$, the loop shape, but only on m , its scale, which can be defined as the square root of the inverse of the area. Two dimensional YM has a dimensional coupling which does not renormalize and simply keeps track of dimensions. The issue of renormalization does not arise at all. We may as well regard the area as dimensionless and set the coupling constant to unity. The dimensionless positive parameter t of the random matrix model corresponds to this dimensionless area. It is convenient to change notation, from t to b ,

$$b = \frac{4}{t} \quad (4.3)$$

and view b as m^2 in our discussion above. $m_c = 1$, since $t_c = 4$. When m increases the loop shrinks.

We can now summarize our previous findings in two dimensions as follows: Consider

$$\tilde{O}_N(y, b) = \left(\frac{N}{12} \right)^{\frac{1}{4}} \sqrt{\frac{2\pi}{Nb}} \frac{e^{\frac{N}{2b}}}{2^N} \left\langle \det \left(e^{\frac{y}{2}} + e^{-\frac{y}{2}} \prod_{i=1}^N U_i \right) \right\rangle \quad (4.4)$$

\tilde{O} is proportional to O but the normalization is b dependent. The large N universal content is independent of the prefactor, so long as the normalization is smooth in b at the point $b = b_c$; therefore the difference between \tilde{O} and O is immaterial. Using (3.19), we can see that

$$\tilde{O}_N(y, b) = \left(\frac{N}{12}\right)^{\frac{1}{4}} \int d\rho e^{N[\ln \cosh \rho - \frac{b}{8}(2\rho - y)^2]}. \quad (4.5)$$

Defining ξ and α by

$$y = \left(\frac{4}{3N^3}\right)^{\frac{1}{4}} \xi; \quad b = 1 + \frac{1}{\sqrt{3N}}\alpha \quad (4.6)$$

and expanding in $\frac{1}{\sqrt{N}}$, we obtained:

$$\lim_{N \rightarrow \infty} \tilde{O}_N(y, b) = \zeta(\xi, \alpha) = \int du e^{-u^4 - \alpha u^2 + \xi u} \quad (4.7)$$

This is how the universality hypothesis is realized in two dimensions, by construction.

4.2 Lattice formulation – completely defined.

Several of the choices we shall make are not conceptually essential, but they help streamline the discussion.

4.2.1 Shape and scale of curves on the lattice.

We start by replacing space-time by a hypercubic lattice in d dimensions. This hypercubic lattice will be viewed as dimensionless, a collection of vertices, or sites, labeled by $x_\mu \in Z, \mu = 1, \dots, d$, and the shortest arcs, or links, connecting them. One adds an orientation to the links: this means that a link parallel to the μ -axis $\mu = 1, \dots, d$ can be traversed in the direction of its orientation ($+\mu$), or in the opposite sense ($-\mu$). This setup is used to define approximations to curve shapes. The curve shape is replaced by a contiguous sequence of links, where the angles between any two links have to be a multiple of ninety degrees. Symbolically, the curve is represented by an ordered sequence, $(\mu_1, \mu_2, \dots, \mu_L)$ where $\mu_i = -d, -(d-1), \dots, d-1, d$. The curve is closed when $\sum_{i=1}^L \delta_{\nu, \mu_i} = 0$ for $\nu = 1, 2, \dots, d$. When the curve is closed there is a redundancy under cyclic shifts of the sequence. The curve is non-self-intersecting if every site is visited no more than once. The total number of links, L , determines how good the approximation is. In the continuum limit one needs to take L to infinity.

A scale parameter is attached to the curve shape by the “dynamics”. To each link we attach an $SU(N)$ unitary matrix U . There is a joint probability distribution for all link matrices U , which is parameterized by a positive parameter that we again call b . The mass scale m is determined by b and the relationship is monotonic: $m(b) \rightarrow 0$ as $b \rightarrow \infty$. The continuum limit is obtained by taking $L \rightarrow \infty, b \rightarrow \infty$, in such a way that $m(b)L = l$ stay finite. One can then arbitrarily introduce a unit of length to give l engineering dimensions.

For a fixed continuum curve, its shape $\mathcal{C}(\ast)$ is obtained from the lattice sequence in the limit when $L \rightarrow \infty$. Simultaneously with that limit one needs to take $b \rightarrow \infty$, while the product $m(b)L = l$ stays finite. l determines the scale of the curve \mathcal{C} , and plays the role of

the parameter $\frac{1}{m}$ in the continuum discussion. One way to investigate what happens as the continuum scale m goes through its critical value for a given curve shape, is to vary b at a fixed lattice curve with a fixed L . The universality hypothesis makes a prediction about this behavior; this prediction is approximate in that the parameters a_1, a_2 are L dependent but becomes accurate as $L \rightarrow \infty$. The order of the limits $L \rightarrow \infty$ and $N \rightarrow \infty$ is assumed to not matter, although there are some limitations on the ranges.

4.2.2 Regularization of perimeter and corner divergences.

To make the prediction of universality quantitative we need to assure that the lattice version of $O_N(y, b)$ is well defined and has a finite continuum limit. We need to eliminate corner and perimeter divergences. They are eliminated by replacing the link matrices U in the standard definition of W by smeared versions, denoted by $U^{(n)}$, where n is an integer.

We employ APE smearing [9], defined recursively from $n = 0$, where the smeared matrix is equal to $U_\mu(x)$. Let $\Sigma_{U_\mu^{(n)}(x;f)}$ denote the ‘‘staple’’ associated with the link $U_\mu^{(n)}(x; f)$ in terms of the entire set of $U_\nu^{(n)}(y; f)$ matrices. One step in the recursion takes one from a set $U_\mu^{(n)}(x; f)$ to a set $U_\mu^{(n+1)}(x; f)$:

$$\begin{aligned} X_\mu^{(n+1)}(x; f) &= (1 - |f|)U_\mu^{(n)}(x; f) + \frac{f}{2(d-1)}\Sigma_{U_\mu^{(n)}(x;f)} \\ Y_\mu^{(n+1)}(x; f) &= X_\mu^{(n+1)}(x; f) \frac{1}{\sqrt{[X_\mu^{(n+1)}(x; f)^\dagger X_\mu^{(n+1)}(x; f)]}} \\ U_\mu^{(n+1)}(x; f) &= \frac{Y_\mu^{(n+1)}(x; f)}{\det^{\frac{1}{N}} [Y_\mu^{(n+1)}(x; f)]} \end{aligned} \quad (4.8)$$

In the simulation, one never encounters a situation where the unitary projection in the above equations stalls because $X^{(n)}$ is singular. In other words, smearing is well defined with probability one.

$U_\mu^{(n)}(x; f)$ transforms under gauge transformations the same way as $U_\mu(x)$ does. For definiteness we restrict our subsequent discussion to rectangular loops of sides L_1 and L_2 which fit into a two dimensional plane in the d dimensional Euclidean space time.

Our smeared Wilson loop operators, $\hat{W}[L_1, l_2; f; n]$ are defined as ordered products around the $L_1 \times L_2$ rectangle restricted to a plane. L_α are integers and give the size of the loop in units of the lattice spacing. When the traversed link starts at site $x = (x_1, x_2, \dots, x_d)$ $x_\mu \in Z$ and connects to the neighboring site in the positive direction μ , $x + \mu$, the link matrix is $U^{(n)}(x; f)$, while when this oriented link is traversed in the opposite direction, the link matrix is $U^{\dagger(n)}(x; f)$. \hat{W} depends on the place the loop was opened, but its eigenvalues do not. The set of eigenvalues is gauge invariant under the fundamental gauge transformation operating on $U_\mu(x)$.

We adjust the parameter dependence in \hat{W} such that the $N = \infty$ transition points which are seen to occur on the lattice, survive in the continuum limit in which the lattice coupling b is taken to infinity together with $L_{1,2}$ in such a way that the physical lengths $l_\alpha = L_\alpha m(b)$ are kept fixed. ($l_1/l_2 = L_1/L_2$ is independent of b , and represents the loop shape; our previously defined scale l is $l = 2m(b)(L_1 + L_2)$).

We set the number of smearing steps n to be proportional to the perimeter square (we restricted the loop sizes to even $L_1 + L_2$), $n = \frac{(L_1+L_2)^2}{4}$. The physical sizes of the loop are l_α . We have set $n = \frac{(L_1+L_2)^2}{4}$ because in physical terms the product fn is a length squared. This is because smearing is a random walk that fattens the loop and the thickness grows as the square root of the number of smearing steps. Our choice for n makes f a dimensionless parameter in the physical sense; on the lattice f is actually bounded to an interval of order one. The effect of smearing is easy to understand in perturbation theory where one supposes that each individual step in the smearing iteration can be linearized. Writing $U_\mu^{(n)}(x; f) = \exp(iA_\mu^{(n)}(x; f))$, and expanding in A_μ one finds [10], in lattice Fourier space:

$$A_\mu^{(n+1)}(q; f) = \sum_\nu h_{\mu\nu}(q) A_\nu^{(n)}(q; f) \quad (4.9)$$

with

$$h_{\mu\nu}(q) = f(q) \left(\delta_{\mu\nu} - \frac{\tilde{q}_\mu \tilde{q}_\nu}{\tilde{q}^2} \right) + \frac{\tilde{q}_\mu \tilde{q}_\nu}{\tilde{q}^2} \quad (4.10)$$

where $\tilde{q}_\mu = 2 \sin(\frac{q_\mu}{2})$ and

$$f(q) = 1 - \frac{f}{2(d-1)} \tilde{q}^2 \quad (4.11)$$

The iteration is solved by replacing $f(q)$ by $f^n(q)$, where, for small enough f ,

$$f^n(q) \sim e^{-\frac{fn}{2(d-1)} \tilde{q}^2} \quad (4.12)$$

Much larger loops should not be smeared with an fn factor that keeps on growing as the perimeter squared; rather, for a square loop of side L , for example, the following choice would be appropriate:

$$f = \frac{\tilde{f}}{1 + M^2 L^2} \quad (4.13)$$

Here, M is in lattice units, $M = \Gamma m(b)$. Γ is a hadronic scale chosen so that at the large N transition, Γl is less than 0.01, say.

The new parameter f should be considered as fixed once and for all; its exact value is unimportant so long as it is reasonable. However, if that value is changed by some modest amount the critical loop size will change too. This critical loop size is non-universal; only the fact that such a critical value exists within some reasonable hadronic range is universal.

Smearing provides a means to regularize the basic observable and allows us to proceed finally to the lattice formulation of the large N universality hypothesis. For simplicity, we formulate it only for square Wilson loops, denoting by W the operator constructed from smeared link variables.

4.2.3 Universality hypothesis for square lattice Wilson loops.

We assume to be given a table (the data) with numerical values for the expectation value of

$$O_N(y, b) = \left\langle \det(e^{\frac{y}{2}} + e^{-\frac{y}{2}} W) \right\rangle \quad (4.14)$$

for an $L \times L$ Wilson loop at an inverse 't Hooft rescaled gauge coupling b . The hypothesis says that $O_N(y, b)$ will exhibit critical behavior at $b = b_c(L)$ and $y = 0$ as $N \rightarrow \infty$. There, it will obey large N universality, which means that there exists a $\mathcal{N}(b, N)$, smooth in b at $b = b_c$, such that:

$$\lim_{N \rightarrow \infty} \mathcal{N}(b, N) O_N \left(y = \left(\frac{4}{3N^3} \right)^{\frac{1}{4}} \frac{\xi}{a_1(L)}, b = b_c(L) \left[1 + \frac{\alpha}{\sqrt{3N} a_2(L)} \right] \right) = \zeta(\xi, \alpha) \quad (4.15)$$

$\mathcal{N}(b, N)$ is a normalization factor similar to the one in (4.4).

4.2.4 Large N universality holds already before the continuum limit.

Even at finite $L \geq L_0$, where L_0 is some finite number there will be a large N phase transition in loops. Our hypothesis includes the belief that this transition will be in the DO universality class even before the continuum limit is taken. Thus, for simple enough loops it always makes sense to define $b_c(L), a_1(L), a_2(L)$. If all three parameters approach the continuum limit in the standard manner, then large N universality is a property of the continuum limit.

This is somewhat similar to spontaneous chiral symmetry on the lattice. Using the overlap action for example [11], we can define a pion decay constant at finite lattice spacing, by relating the pion mass for small bare quark masses using standard chiral symmetry considerations. That all this survives the continuum limit amounts simply to checking that physical quantities have smooth limits, approached in standard ways. The key is to have a good lattice definition that preserves the essential ingredient of the phenomenon. When there is no reason, the continuum limits and other critical behaviors do not interfere with each other. However, if the lattice regularization is faulty, for example ignoring perimeter effects in the case of Wilson loops, or choosing a Wilson type of fermionic action in the chiral case, one will have interference with the continuum limit. This is not to say that these problems cannot be overcome –only the analysis becomes more murky and delicate.

4.2.5 How to test for universal large N behavior numerically?

We test for large N universality hypothesis as follows: Obtain estimates for $b_c(L), a_1(L), a_2(L)$ denoted by $b_c(L, N), a_1(L, N)$ and $a_2(L, N)$ from data at various values of N assuming N is already large enough to use the asymptotic formulas.

- Show that all three N -dependent quantities have a well defined limit as $N \rightarrow \infty$, which is approached in a way consistent with large N universality.
- Show that $b_c(L), a_1(L), a_2(L)$ have finite limits as $L \rightarrow \infty$ (which are correlated with taking $b \rightarrow \infty$ keeping the physical loop size fixed). Moreover, these limits should be approached in the manner expected of normal physical field theoretical observables (that is the sub-leading corrections can be organized by dimensional analysis restricted by symmetry considerations).

4.2.6 The estimates $b_c(L, N)$ for $b_c(L)$.

$O_N(y, b)$ is an even function of y because $W \in SU(N)$. It is obvious from (4.7) that $\zeta(\xi, \alpha)$ is an even function of ξ . Let

$$O_N(y, b) = C_0(b, N) + C_1(b, N)y^2 + C_2(b, N)y^4 + \dots \quad (4.16)$$

be the Taylor's series for $O_N(y, b)$. At some fixed value of L we consider the following quantity, derived from the average characteristic polynomial of the regularized Wilson loop:

$$\Omega(b, N) = \frac{C_0(b, N)C_2(b, N)}{C_1^2(b, N)}. \quad (4.17)$$

$\Omega(b, N)$ is essentially a ‘‘Binder cumulant’’ [12]. The normalization $\mathcal{N}(b, N)$ and any rescaling of y drop out from $\Omega(b, N)$. Therefore, if N is large enough, and if we set $b = b_c(L, N = \infty)$ we should get a value close to the number $\Omega(b_c, \infty)$. We define an approximation to $b_c(L, N = \infty)$, $b_c(L, N)$, by the equation:

$$\Omega(b_c(L, N), N) = \frac{\Gamma(\frac{5}{4})\Gamma(\frac{1}{4})}{6\Gamma^2(\frac{3}{4})} = \frac{\Gamma^4(\frac{1}{4})}{48\pi^2} = 0.364739936 \quad (4.18)$$

Viewing the u integrand in (4.7) as performing an average over u dependent observables, we would write, $C_k = \frac{\langle u^{2k} \rangle}{(2k)!}$. For $|\alpha| \gg 1$ we can assume that u is approximately distributed as a Gaussian. For $\alpha > 0$ the mean is zero, $\langle u \rangle = 0$, and using $\frac{\langle u^4 \rangle}{\langle u^2 \rangle^2} = 3$ gives $\Omega = \frac{1}{2}$. If $\alpha < 0$ there are two nonzero saddles of the same absolute magnitude $\langle u \rangle \neq 0$; these saddles dominate over fluctuations, giving $\Omega = \frac{1}{6}$. The full function $\Omega(\alpha)$ is shown in Figure 2.

At $\alpha = 0$ Ω comes out pretty close to the arithmetic average of the two asymptotic values: $\frac{1}{2}(\frac{1}{2} + \frac{1}{6})$. The exact number is given in (4.18); it was obtained from (4.7) using

$$\int_{-\infty}^{\infty} du u^{2k} e^{-u^4} = \frac{1}{2} \Gamma\left(\frac{2k+1}{4}\right) \quad (4.19)$$

Expanding $\tilde{O}(y, b)$ in (4.5) to order y^4 leads to explicit expression for $\Omega(b, N)$. Figure 3 shows $\Omega(b, N)$ for different values of N . In two dimensions the exact $\Omega(b, N)$ connects monotonically the two extremes, $1/6$ and $1/2$ as b varies from far below b_c to far above b_c . If one takes $N \rightarrow \infty$, there is a discontinuous jump at $b = b_c$, between the above two asymptotic values. The double scaling limit of $\Omega(b, N)$, which produced $\Omega(\alpha)$, smoothed out the jump but maintained the asymptotic behavior of the exact expression at finite N .

From the data we get estimates of $C_i(b, N)$, $i = 0, 1, 2$, from which we extract $\Omega(b, N)$. We then use (4.18) to obtain an estimate of $b_c(L, N)$.

$b_c(L, N)$ has been constructed from the free energy of the combined system of gauge fields and fermions used to represent the characteristic polynomial. Therefore, ordinary N -power counting rules should apply, and we expect $b_c(L, N)$ to approach $b_c(L, \infty) \equiv b_c(L)$ as a series in $\frac{1}{N}$.

4.2.7 The estimates $a_2(L, N)$ for $a_2(L)$.

The parameter $a_2(L, N)$ is obtained by first setting

$$b = b_c(L, N) \left[1 + \frac{\alpha}{\sqrt{3N} a_2(L, N)} \right], \quad (4.20)$$

where $b_c(L, N)$ has been defined above. Next we write the derivative of Ω with respect to α and set the result equal to the corresponding universal number in the large N limit.

$$\left. \frac{d\Omega(b, N)}{d\alpha} \right|_{\alpha=0} = \frac{1}{a_2(L, N) \sqrt{3N}} \left. \frac{d\Omega}{db} \right|_{b=b_c(L, N)} = \frac{\Gamma^2(\frac{1}{4})}{6\sqrt{2}\pi} \left(\frac{\Gamma^4(\frac{1}{4})}{16\pi^2} - 1 \right) = 0.0464609668 \quad (4.21)$$

$\frac{d\Omega}{db}$ would be close to maximal at $b = b_c$; hence $\frac{d\Omega}{db}$ varies relatively little as b stays close to b_c . Since b_c is not known to infinite accuracy the reduced sensitivity on the exact value of b_c is an advantage which motivates this choice for defining $a_2(L, N)$. Unlike $b_c(L, N)$, the definition of $a_2(L, N)$ involves going into the large N critical regime around $b_c(L, \infty)$ and non-standard powers of N come in. Taking this into account, we expect $a_2(L, N)$ to approach $a_2(L, \infty) \equiv a_2(L)$ as a power series in $\frac{1}{\sqrt{N}}$.

4.2.8 The estimates $a_1(L, N)$ for $a_1(L)$.

We substitute

$$y = \left(\frac{4}{3N^3} \right)^{\frac{1}{4}} \frac{\xi}{a_1(L, N)} \quad (4.22)$$

in (4.16). We then form a ratio whose value at infinite N is again a universal number we can easily compute.

$$\sqrt{\frac{4}{3N^3}} \frac{1}{a_1^2(L, N)} \frac{C_1(b_c(L, N), N)}{C_0(b_c(L, N), N)} = \frac{\pi}{\sqrt{2}\Gamma^2(\frac{1}{4})} = 0.16899456 \quad (4.23)$$

This relation defines $a_1(L, N)$.

Similarly to $a_2(L, N)$, the definition of $a_1(L, N)$ involves going into the large N critical regime around $b_c(L, \infty)$. Consequently, we expect $a_1(L, N)$ to also approach $a_1(L, \infty) \equiv a_1(L)$ as a power series in $\frac{1}{\sqrt{N}}$.

4.3 Example of a universality test on synthetic two dimensional data.

In two dimensions we work already in the limit $L = \infty$. Our main objective is to check what kind of finite N data could be used to produce the known infinite N values of a_1, a_2, b_c , using the above procedures (with L eliminated) to define $a_1(N), a_2(N), b_c(N)$. The extrapolation to infinite N is done using a series in $\frac{1}{N}$ for $b_c(N)$ and a series in $\frac{1}{\sqrt{N}}$ for $a_1(N), a_2(N)$ as explained above. The values of N in Figure 3 were chosen to match the ones employed in the three dimensional simulation.

$\Omega(b, N)$, as a continuous function of b for a fixed N , defines via (4.18) the number $b_c(N)$. With $b_c(N)$ so determined, we use (4.21) to determine $a_2(N)$ from $\left. \frac{d\Omega(b, N)}{db} \right|_{b=b_c(N)}$. Further, we use (4.23) to find the value of $a_1(N)$ from $\frac{C_1(b_c(N), N)}{C_0(b_c(N), N)}$. Figures 4,5,6 show what

can be done with “perfect” data for $N = 17, 23, 29, 37, 41, 47$. The $N \rightarrow \infty$ estimate of b_c is the most accurate followed by the estimates of a_1 and a_2 . This is typical in that we expect (and need) an accurate estimate of the critical point while the estimate of the amplitudes come at lower accuracy.

While the synthetic data was produced only at values of N that are practical also in three dimensions, it has three features that are not in common with lattice data obtained by Monte Carlo simulations:

1. There are no statistical errors.
2. We know $\Omega(b, N)$ and $\frac{C_1(b_c(N), N)}{C_0(b_c(N), N)}$ as continuous functions of b . The numerical simulation will be performed only on a discrete set of b values that brackets $b_c(N)$ and one will need to interpolate.
3. We know $\frac{d\Omega(b, N)}{db}$ exactly. A direct numerical estimate of this derivative would involve linear combinations of connected correlations of $C_i(b, N)$ with the plaquette operator. This has large statistical errors and is expected to be too expensive to compute accurately. Therefore, we shall not have a direct numerical estimate of the derivative and will extract it from the interpolation of $\Omega(b, N)$ we have already used when determining $b_c(N)$.

The synthetic data is used to indicate to us what ranges of N are needed to reliably extrapolate the three parameters to their $N \rightarrow \infty$ limits. The conclusion is that it is possible to carry out quite accurate estimates of b_c and reasonably accurate estimates of a_2 and a_1 in that $N \rightarrow \infty$ limit from data obtained at values of N which are within the range of Monte Carlo simulations in dimensions higher than two. However, the differences we have listed above are sources of extra systematic and stochastic errors that we shall need to control.

4.4 Volume dependence and large N reduction.

In a precise sense, YM theory in 3 or 4 dimensions on a finite torus becomes independent of torus size at infinite N if the torus is larger than some critical torus [13]. The size has to be large enough for the system to be in the so called 0c phase at infinite N . In 0c, traces of Wilson loops in representations of finite dimension are equal to their infinite volume values up to corrections of order $\frac{1}{N^2}$. 0c is characterized by all Polyakov loops having uniform eigenvalue distributions. Using the fermionic representation of the average characteristic polynomial we expect that

$$\frac{1}{N} \log(\langle \det(z - W) \rangle) \tag{4.24}$$

will also be independent of the volume at leading order at large N , with corrections going as $\frac{1}{N}$. Looking at the powers of N that enter into the function $\zeta(\xi, \alpha)$ we conclude that it also should be independent of the volume. However, one expects the sub-leading corrections in $\frac{1}{N}$, which are volume dependent (and non-universal even at infinite volume) to be relatively larger than for traces of Wilson loops. The reason to expect slower convergence to the infinite N limit is that $\zeta(\xi, \alpha)$ describes a large N critical regime, where taking enough

derivatives with respect to some parameter would produce quantities that diverge in the ordinary (without double scaling) large N limit. Obviously, nothing is supposed to diverge at finite N , so sub-leading corrections must be large. These sub-leading corrections will be even more significant at smaller volumes.

Thus, although large N reduction can be exploited, one needs to carry out an explicit check to determine how much contamination of the final estimates has been caused by using relatively small volumes.

5. Three dimensions.

We use an ordinary single plaquette Wilson action defined on a hypercubic lattice. Our simulation method employs a combination of heat-bath and over-relaxation updates and “thermal equilibrium” is achieved in reasonable lengths of computer time. We keep our statistical errors small relative to systematical ones. Throughout, we use b for the lattice gauge coupling which is the inverse bare ’t Hooft coupling. It is related to the conventional lattice coupling β by

$$b = \frac{\beta}{2N^2} = \frac{1}{g_{\text{YM}}^2 N} \quad (5.1)$$

and b already has the right power of N extracted. It is useful to consider the tadpole improved coupling, $b_I = be(b)$ where $e(b)$ is the average value of the trace of plaquette operator. To facilitate a translation from b to b_I , we have plotted $e(b)$ in Figure 7 for the range of b used in this paper.

We started the project by carrying out preliminary simulations, intended to identify a convenient value for the parameter f . We established, in a way similar to our earlier work in four dimensions [1], that as $L_1 = L_2 = L$, f, n are varied, at specific lattice couplings, the spectrum of $\hat{W}[L_1 = L_2 = L; f; n]$ opens a gap for very small and/or very smeared loops. This gap closes for very large and/or very lightly smeared loops. We worked¹ at $N = 37$ on a 8^3 lattice. Keeping b fixed, we varied f and obtained an estimate of the gap using the technique described in [1]. This was done for several Wilson loops of size L^2 , L ranging from $L = 2$ to $L = 10$. In this manner, we obtained estimates for $f_c(L, b)$, the critical value of f at which the gap opens around eigenvalue -1 when the smearing of $L \times L$ Wilson loops is steadily increased at fixed b . The function $f_c(L, b)$ has a continuum limit, obtained when L and b go to infinity in the usual correlated way. This was tested employing five different values of coupling, $b = 0.85, 0.9, 1.0, 1.1, 1.2, 1.3$; we made sure that all these couplings are in the $0c$ phase [14] for our 8^3 lattice. We found that all the values $f_c(L, b)$ fall on a common curve when plotted as a function $L/b_I(b)$ as shown in Figure 8.

Based on this work, we chose to carry out the more detailed analysis of the large N critical region, which is the main topic of this paper, at $f = 0.03$. Other values of f , between 0.02 and 0.04, might have served as well, although many numbers, including b_c and a_2 , would have changed by modest amounts. Much higher values of f are counter indicated at this stage of our research because we want to avoid finite volume effects and

¹We would like to thank Alejandro de la Puente for some preliminary work in this direction.

therefore wish to keep L below 8. A lattice of size 8^3 affords reasonably speedy simulation, even at $N = 47$, but the cost quickly escalates when the lattice size is increased. A more detailed discussion of finite size effects will be presented below.

5.1 Details of the numerical analysis.

Our simulations are carried out for prime numbers for N to ensure that the phase 0c does not decay into phases related to proper subgroups of $Z(N)$. This is a precaution; it is possible that one could also work with non-prime values of N . We employed six different values of N , namely $N = 17, 23, 29, 37, 41, 47$. There are three more primes in this range, but they are so close to other primes, that we did not expect the extra information to be worth the effort. In order to check for volume dependence we obtained data for 2^2 Wilson loops on $3^3, 4^3$ and 6^3 lattices and for the 3^2 loop on 4^3 and 8^3 lattices. For our main study of the double scaling limit we produced data for loops of larger sizes, $4^2, 5^2$ and 6^2 , all on a single lattice size, 8^3 . For each square loop L^2 , and for each value of N we carried out a series of simulations in a range of b separated by small steps Δb . Table 1, which provides the intermediate numerical output used in the study of the double scaling limit, also lists all values of L and N along with the lattice volume V .

After equilibration, for which we typically allowed several thousands of lattice passes, the different steps were separated by 1000 passes. We tested the autocorrelation for our observable and saw that we exceeded it by enough not to have to worry about the independence of our samples. For each entry in the Table 1 we did somewhere between 31 to 48 separate simulations on parallel nodes in one of our PC clusters. Measurements on a single Wilson loop was averaged over the whole lattice for all orientations. Statistical errors obtained from the measurements on several configurations were always estimated by jackknife with single elimination.

In each run we collected data for 30 values of y around zero, at equally spaced points, where the range was determined to be fixed in terms of the corresponding rescaled ξ variable, assuming $a_1 = 1$ at all N, L and b : $0 \leq \xi \leq 3$. There is no need to collect data also at negative values of ξ , since the symmetry under a sign flip of y is exact.

In order to perform a cross-check of our procedure described in (4.2.6), (4.2.7) and (4.2.8), the first type of data we collected is for the observable $O(y, b, L)$:

$$O(y, b, L) = \langle \det \left(e^{\frac{y}{2}} + e^{-\frac{y}{2}} W(b, L) \right) \rangle \quad (5.2)$$

More specifically, we collected data for its logarithmic derivative with respect to y directly; this means that at fixed y, b, L for each gauge configuration and for each loop one keeps two numbers, the determinant and its derivative with respect to y . These numbers are summed over all translations of the loop and these two numbers are stored for subsequent gauge averaging when the analysis is done. For a fixed N and L , the data makes up a two dimensional rectangular grid in the ξ, α plane.

We used a nonlinear fitting routine to find a best match of the logarithmic derivative with respect to y of O to the logarithmic derivative with respect to ξ of the double scaling function $\zeta(\xi, \alpha)$. This produces three parameters $b_c(L, N), a_1(L, N), a_2(L, N)$ which can be

extrapolated later on, first in N , and subsequently in L . The fitting routine we used was based on the Levenberg-Marquart method and the implementation in [15]. The logarithmic derivative with respect to ξ of the double scaling function $\zeta(\xi, \alpha)$ was calculated using gaussian integration over several intervals to high accuracy. In addition to producing estimates to the parameters as mentioned, this showed us that indeed one approaches the double scaling limit. We first tested the nonlinear fitting method on synthetic data in two dimensions as reported in [16]. This will not be reviewed here again. As a method of estimating parameters, the simultaneous nonlinear fit has the drawback that all parameters now have corrections of the order $\frac{1}{\sqrt{N}}$. As we have seen, for $a_1(L, N), a_2(b, N)$ this is unavoidable, but for $b_c(L, N)$ we can do better. The nonlinear simultaneous fit mixes the corrections up and therefore is not the best way to prepare the ground for the large N extrapolation.

The second type of data we collected is used for determining the parameters from the behavior around $y = 0$ that are expressed by the three coefficients $C_i(b, N, L)$.

We first obtain an estimate for $\Omega(b, N, L)$. Figure 9 shows a sample plot of $\Omega(b, N, L)$ as a function of b for $N = 47$ and $L = 3$ on a 4^3 lattice. The behavior is similar to the two dimensional case. The top and bottom horizontal lines are the limits at weak and strong coupling, $1/2, 1/6$ respectively. The middle line is the expected value at critical coupling in the $N \rightarrow \infty$ limit as given by the right hand side of (4.18).

We focus on a region of $\Omega(b, N, L)$ that is bounded by the two horizontal lines that are on either side of the middle line in Figure 9. We view b as a function of $z = \Omega(b, N, L) - 0.364739936$ in this region and use a linear three-parameter fit to a degree 2 polynomial:

$$b = b_c(L, N) + \frac{1}{\left. \frac{d\Omega}{db} \right|_{b=b_c(L, N)}} z + \beta z^2 \quad (5.3)$$

This gives us our determination for $b_c(L, N)$. With the help of this same polynomial we then extract $a_2(L, N)$, using (4.21).

Next, we analyze the numbers for the ratio $\frac{C_1(b, N, L)}{C_0(b, N, L)}$ as follows: We take $\frac{C_1(b, N, L)}{C_0(b, N, L)}$ as a function of z in the same region we used above and again carry out a linear three-parameter fit to a degree 2 polynomial. $\frac{C_1(b_c(L, N), N, L)}{C_0(b_c(L, N), N, L)}$ is set as the leading coefficient in this fit. Finally, $a_1(L, N)$ is extracted using equation (4.23).

5.2 Extrapolation to infinite N .

We take the 6^2 loop on 8^3 lattice as a sample case and plot the results from the linear fit using described in (4.2.6), (4.2.7) and (4.2.8). The solid circles in figures 10,11 and 12 show the results for $b_c(L, N)$, $a_2(L, N)$ and $a_1(L, N)$ respectively. The extrapolation to infinite N was done using a three term series. One cannot use smaller N value when doing this and larger N values are two expensive in computer time to produce, the simulation time growing as N^3 . Some systematic errors are induced by this extrapolation; one can get a feel for it by using more, or less, powers of N in the series. The open circles in figures 10,11 and 12 show the performance of the fit finite N numbers and their infinite N extrapolated values. The $N = \infty$ estimate differs from the data at the largest N by 6%, 39% and 10% for b_c , a_2 and a_1 respectively. This amount of extrapolation is roughly the same as that we had

in the analysis of the synthetic two dimensional data except for a_2 , where it is around 20% for the synthetic data. All in all, although the extrapolations are quite substantial, they are in line with expectations, and the two dimensional study provides some confidence in the validity of the infinite N numbers we obtained in three dimensions. The sample case we show is typical of other loops we have analyzed. Always, the determination of $b_c(L, \infty)$ is the most reliable. Next in terms of reliability is the determination of $a_1(L, \infty)$. The determination of $a_2(L, \infty)$ is the least reliable, perhaps because of an amplification of small errors in the determination of $b_c(L, \infty)$.

As a cross-check of the determination of the infinite N numbers we analyze the 6^2 loops also using the nonlinear simultaneous three parameter fit we described earlier. We compare our three target numbers, $b_c(L, \infty)$, $a_1(L, \infty)$ and $a_2(L, \infty)$ obtained in the nonlinear simultaneous fit to those obtained in the linear method based on Ω .

It is only the infinite N values that have to agree within errors, since finite N effects will differ in the two methods. We do not make a great effort to estimate the errors in the nonlinear fit, as it is used only for a general consistency test. We observe a dependence on the ranges we use which produces systematic errors that are larger than the statistical ones. It is this dependence on ranges we eliminate in large measure (not completely though, as we need a range of b -values for interpolation purposes, as explained) in the linear fitting method, based on Ω . But, one may worry that focusing on too narrow a range in b can do more harm than good. This is the intuitive reason for our carrying out this consistency test. It goes above the usual feeling that nonlinear multi-parameter fits are less reliable than sequential linear fits.

The results from the nonlinear simultaneous fit are shown by solid triangles in Figures 10,11 and 12. The open triangles show the performance of the fit versus N and also show the extrapolated values at infinite N . As expected, they do not agree at finite N , but there is reasonable agreement on the extrapolated values at $N = \infty$. This assures us that focusing on the region at $y = 0$ in the linear method based on Ω does not present any dangers to reliability.

The method used for fitting the parameters, as we have explained before, deals with one parameter at a time and indirectly uses linear fits. This is our main method and it gave three numbers for each V, L, N , which are summarized in Table 1

5.3 Finite volume effects.

As explained, one needs to test for contamination from finite volume effects, even though there is large N reduction promising an eventual lack of sensitivity to finite volume effects. It is not that the true infinite N values are suspected of being dependent on torus size: The point is that the estimates we get for the infinite N values are obtained by extrapolation from a set of finite N values. Each one of these finite N numbers does have a torus size dependence. Fitting to this finite set of values at finite N 's will produce best fit parameters that will depend on torus size too. The parameter giving the coefficient of $\frac{1}{N^0}$ will have some torus size dependence too, which would get weaker as more data at higher values of N is made available. The coefficients of sub-leading terms of the form $\frac{1}{N^k}$, $k > 0$ will have a dependence on torus size that is not supposed to disappear when data at higher values

of N is made available. In any finite set of data, the coefficient of $\frac{1}{N^0}$ will compensate, by some torus size dependence, for the absence of data at even higher values of N .

We have tested for contamination from finite volume effects in two cases: We compare in Figures 13,14 and 15 the results obtained using a 4^3 and a 8^3 volume for a 3^2 loop and 3^3 , 4^3 and 6^3 volumes for a 2^2 loop. We see that only smaller values of N are affected. Also, the effect is stronger on the 3^2 loop, which makes sense since 3^2 loop on a 4^3 volume ought to be more contaminated than a 2^2 loop on a 3^3 volume. However, the main conclusion is positive: our infinite N values are safe at our level of accuracy from finite volume contamination.

5.4 Extrapolation to infinite L – continuum extrapolation.

The transition is a continuum feature; therefore, all the values of L represent the same critical loop of a physical size l_c . In three dimensions b has dimensions of length, therefore $\frac{L}{b_c(L)}$ needs to approach a finite limit. This limit is to be approached with corrections dictated by renormalization theory. Although the action generates only dimension two corrections, the observable has also dimension one corrections, and therefore all our fits are to three terms in a series in $\frac{1}{L}$ for $\frac{b_c}{L}$, a_1 and a_2 . Higher L values run the danger of finite volume contamination and therefore we avoided producing them. There also is a cost factor involved since the higher L is the larger the lattice b is and consequently the larger the lattice volume has to be in order to stay in the right phase, $0c$. As usual, computer time will eventually grow linearly with L^3 .

One way to check for consistency is to redo the fits by replacing the values $b_c(L)$ for each L by their mean field, or tadpole, improved values:

$$b^I(b) = be(b) \tag{5.4}$$

where $e(b)$ is the average of $\frac{\text{Tr}(U_p)}{N}$ for unsmeared parallel transporters round plaquettes p . It is known that a large fraction of $\frac{1}{b^2}$ corrections get absorbed when using b^I instead of b as an extrapolation parameter to continuum. If our continuum extrapolation method is to be more than merely asserted, it should give almost the same numbers in the continuum limit when using either extrapolation method. However, when using mean field improvement we should see less fractional variability as function of L . These features were indeed observed; thus our continuum extrapolation has passed a self-consistency check, which admittedly is somewhat heuristic.

Figures 16,17 and 18 show how the continuum limit is approached. The 2×2 loop is probably on too coarse a lattice and we perform fits which include and fits which exclude this loop. Figure 16 shows the results for $\frac{b_c(L,\infty)}{L}$ and $\frac{b_{cI}(L,\infty)}{L}$. The extrapolated value for both data sets are consistent with each other but there is a significant difference in the extrapolated value with and without the 2×2 loop. The χ^2 value indicates that probably the lattice spacing for the 2^2 loops becomes too large. We therefore quote 0.113(6) as the continuum value for b_c/l at $f = 0.03$. The extrapolated result for a_2 has large errors as expected and all we can quote is 5.8(2.3). The result for a_1 is consistent with a_1 being unity.

6. Summary and Discussion.

We hypothesized that the strong to weak coupling phase transition in large N QCD is in the same universality class in two, three and four dimensions. Our primary finding is a picture that is consistent with our hypothesis in three dimensional Euclidean YM. Moreover, it seems that the parameter a_1 is consistent with the value 1, indicating that indeed the phase transition is as simple as it only could be.

One should keep in mind that numerical tests are never foolproof. Even if it turns out that some details do not work as the hypothesis we formulated predicts, there could be weaker forms of the hypothesis that do hold. We believe that it is better to have some clear hypothesis one is testing, than just trying to accumulate a large body of numerical information and look for systematics later. We hope that our hypothesis, or a competing one, will be independently checked in perhaps other ways.

7. Plans for the future.

The first problem for the future is to extend this work to four dimensions. If everything works like in three dimensions one can proceed to address the question of shape dependence.

It would be useful to derive double scaling limits for observables other than the characteristic polynomial and use those for carrying out numerical tests. In particular, the double scaling limit of the distribution of extremal eigenvalues would hold the promise of providing easier and more stringent numerical checks.

A related question has to do with matching the universal data in the transition region to the perturbative side. For this, smearing and the precise form of the observable become important practical details. Intuitively, the Grassmann/fermion representation for the characteristic polynomial provides a framework that has better potential to be amenable to standard renormalized perturbation theory than whatever framework would be able to handle extremal eigenvalues. The reason is that the Grassmann/fermion representation provides local expressions in spacetime, but it is hard to imagine a space-time local approach for handling a double scaling limit for the distribution of extremal eigenvalues. Nevertheless, exact results about extremal eigenvalues would be useful, only, one may need to match (this time within the matrix model) the parametric behavior of extremal eigenvalues (assuming one can be obtained) to the description of the average characteristic polynomial we have been working with in this paper.

The concept of an extremal eigenvalue is less natural for a unitary matrix than it is for a hermitian one. In the unitary case, one would define “extremal” by the eigenvalue on the unit circle that is closest to -1, the distance being measured by the shortest arc connecting the eigenvalue to -1 round the unit circle. Perhaps a more natural alternative is to consider the probability distribution of the largest gap, where the “gaps” are measured by arcs connecting two consecutive eigenvalues round the circle.

Acknowledgments

R.N. acknowledge partial support by the NSF under grant number PHY-055375. H. N.

acknowledges partial support by the DOE under grant number DE-FG02-01ER41165 at Rutgers University and a Humboldt Foundation prize. The stay associated with the prize, at Humboldt University Berlin, was very pleasant and H. N. is grateful to Ulli Wolff and his computational physics group for their hospitality during two long-term stays in Berlin. Comments made by J. Feinberg, during an extended visit at Rutgers, are also gratefully acknowledged.

References

- [1] R. Narayanan, H. Neuberger, *JHEP* **03** (2006) 064.
- [2] B. Durhuus and P. Olesen, *Nucl. Phys. B* **184**, 461 (1981).
- [3] A. M. Migdal, *ZhETF (USSR)* **69** (1975) 810 (*JETP (Sov. Phys.)* **42** (1976) 413).
- [4] R. A. Janik, W. Wiecek, *J. Phys. A: Math. Gen.* **37**, 6521 (2004).
- [5] R. Gopakumar and D.J. Gross, *Nucl. Phys. B* **451**, 379 (1995).
- [6] T. D. Lee, C. N. Yang, *Phys. Rev.* **87**, 410 (1952)
- [7] F.A. Berezin, *Teoreticheskaya i Matematicheskaya Fizika*, Vol. **17**, No.3 305 (1973).
- [8] D. V. Voiculescu, K. J. Dykema, A. Nica, “Free Random Variables” AMS — CRM, (1992).
- [9] T. DeGrand, *Phys. Rev. D* **63** (2001) 034503; M. Albanese et. al. [APE Collaboration], *Phys. Lett. B* **192**, (1987) 163; M. Falcioni, M.L. Paciello, G. Parisi and B. Taglienti, *Nucl. Phys. Nucl. Phys.* **B251**, 624 (1985).
- [10] C. W. Bernard and T. DeGrand, *Nucl. Phys. Proc. Suppl.* **83**, 845 (2000).
- [11] H. Neuberger, *Phys. Lett.* **B417** (1998) 141; *Phys. Lett.* **B427** (1998) 353. R. Narayanan and H. Neuberger, *Phys. Lett. B* **616**, 76 (2005); *Nucl. Phys.* **B696**, 107 (2004).
- [12] K. Binder, *Phys. Rev. Lett.* **47**, 693 (1981).
- [13] R. Narayanan and H. Neuberger, *Phys. Rev. Lett.* **91** (2003) 081601; J. Kiskis, R. Narayanan and H. Neuberger, *Phys. Lett.* **B574** (2003) 65.
- [14] R. Narayanan, H. Neuberger, F. Reynoso, *Phys. Lett.* **B651** (2007) 246.
- [15] “Numerical Recipes”, by William H. Press et. al., Cambridge University Press, (1990).
- [16] R. Narayanan, H. Neuberger, arXiv:0709.4494.

V	L	N	$b_c(L, N)/L$	$b_{cI}(L, N)/L$	$a_2(L, N)$	$a_{2I}(L, N)$	$a_1(L, N)$
3^3	2	17	0.2564(3)	0.1578(4)	1.69(3)	0.91(2)	0.831(1)
3^3	2	23	0.2506(3)	0.1508(3)	1.88(4)	0.97(2)	0.846(1)
3^3	2	29	0.2483(3)	0.1479(3)	2.01(6)	1.03(3)	0.855(1)
3^3	2	37	0.2463(3)	0.1454(3)	2.19(5)	1.09(2)	0.863(2)
3^3	2	41	0.2457(3)	0.1447(3)	2.12(5)	1.06(3)	0.866(2)
3^3	2	47	0.2444(3)	0.1433(3)	2.18(6)	1.09(3)	0.872(2)
4^3	2	17	0.2568(2)	0.1581(2)	1.61(2)	0.87(1)	0.832(0)
4^3	2	23	0.2515(2)	0.1517(2)	1.82(2)	0.95(1)	0.845(1)
4^3	2	29	0.2483(2)	0.1479(2)	1.97(3)	1.00(1)	0.856(1)
4^3	2	37	0.2461(2)	0.1452(3)	2.08(4)	1.04(2)	0.864(1)
4^3	2	41	0.2452(2)	0.1441(3)	2.12(4)	1.05(2)	0.868(1)
4^3	2	47	0.2447(2)	0.1435(2)	2.28(5)	1.13(2)	0.871(1)
6^3	2	17	0.2567(1)	0.1579(1)	1.60(1)	0.87(1)	0.832(0)
6^3	2	23	0.2514(1)	0.1516(1)	1.79(1)	0.94(1)	0.846(0)
6^3	2	29	0.2485(1)	0.1481(1)	1.94(2)	0.99(1)	0.855(0)
6^3	2	37	0.2460(1)	0.1451(1)	2.07(2)	1.03(1)	0.865(1)
6^3	2	41	0.2454(1)	0.1443(1)	2.14(2)	1.06(1)	0.868(1)
6^3	2	47	0.2445(1)	0.1433(1)	2.24(2)	1.11(1)	0.872(1)
4^3	3	17	0.2309(3)	0.1695(3)	1.39(2)	0.98(1)	0.838(0)
4^3	3	23	0.2258(3)	0.1641(3)	1.45(2)	1.00(2)	0.854(1)
4^3	3	29	0.2228(2)	0.1608(2)	1.45(2)	1.00(1)	0.866(1)
4^3	3	37	0.2197(2)	0.1575(2)	1.50(3)	1.03(2)	0.878(1)
4^3	3	41	0.2185(2)	0.1564(2)	1.55(2)	1.06(1)	0.883(1)
4^3	3	47	0.2177(2)	0.1554(2)	1.59(4)	1.08(2)	0.888(1)
8^3	3	17	0.2344(1)	0.1731(1)	1.27(1)	0.90(0)	0.838(0)
8^3	3	23	0.2268(1)	0.1652(1)	1.36(1)	0.95(0)	0.855(0)
8^3	3	29	0.2228(1)	0.1609(1)	1.44(1)	0.99(1)	0.867(0)
8^3	3	37	0.2199(1)	0.1578(1)	1.51(1)	1.03(1)	0.878(0)
8^3	3	41	0.2188(1)	0.1566(1)	1.54(1)	1.05(1)	0.883(0)
8^3	3	47	0.2176(1)	0.1554(1)	1.54(4)	1.05(2)	0.889(0)
8^3	4	17	0.2189(1)	0.1741(1)	1.19(1)	0.93(1)	0.839(0)
8^3	4	23	0.2115(1)	0.1665(1)	1.30(1)	1.00(1)	0.856(0)
8^3	4	29	0.2075(1)	0.1624(1)	1.34(1)	1.02(1)	0.868(0)
8^3	4	37	0.2043(1)	0.1591(1)	1.41(1)	1.07(1)	0.880(0)
8^3	4	41	0.2031(1)	0.1578(1)	1.42(1)	1.08(1)	0.885(0)
8^3	4	47	0.2021(1)	0.1568(1)	1.46(1)	1.10(1)	0.890(0)
8^3	5	17	0.2054(1)	0.1701(1)	1.17(1)	0.96(1)	0.839(0)
8^3	5	23	0.1986(1)	0.1631(1)	1.26(1)	1.02(1)	0.856(0)
8^3	5	29	0.1949(3)	0.1594(3)	1.32(2)	1.06(2)	0.869(1)
8^3	5	37	0.1919(1)	0.1563(1)	1.37(1)	1.10(1)	0.880(0)
8^3	5	41	0.1907(1)	0.1551(1)	1.40(4)	1.12(3)	0.887(2)
8^3	5	47	0.1896(1)	0.1540(1)	1.45(2)	1.16(1)	0.892(1)
8^3	6	17	0.1944(2)	0.1652(2)	1.24(1)	1.04(1)	0.839(0)
8^3	6	23	0.1889(2)	0.1597(2)	1.26(1)	1.06(1)	0.856(0)
8^3	6	29	0.1854(1)	0.1561(1)	1.28(1)	1.07(1)	0.868(0)
8^3	6	37	0.1826(1)	0.1532(1)	1.34(1)	1.11(1)	0.881(0)
8^3	6	41	0.1818(2)	0.1524(2)	1.39(3)	1.15(2)	0.885(1)
8^3	6	47	0.1805(1)	0.1512(1)	1.42(2)	1.18(2)	0.892(1)

Table 1: The results for the parameters matching lattice data to the double scaling function at different values of V , L and N .

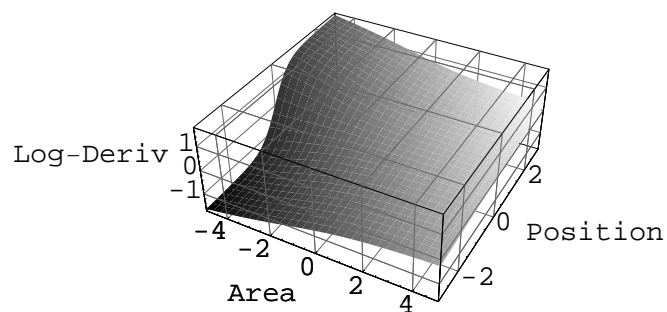


Figure 1: Plot of the logarithmic derivative of ζ with respect to ξ for different values of the “area” (α) and “position” (ξ). One sees the smooth remnant of the singularity at $\xi = 0$ and its dependence on the area.

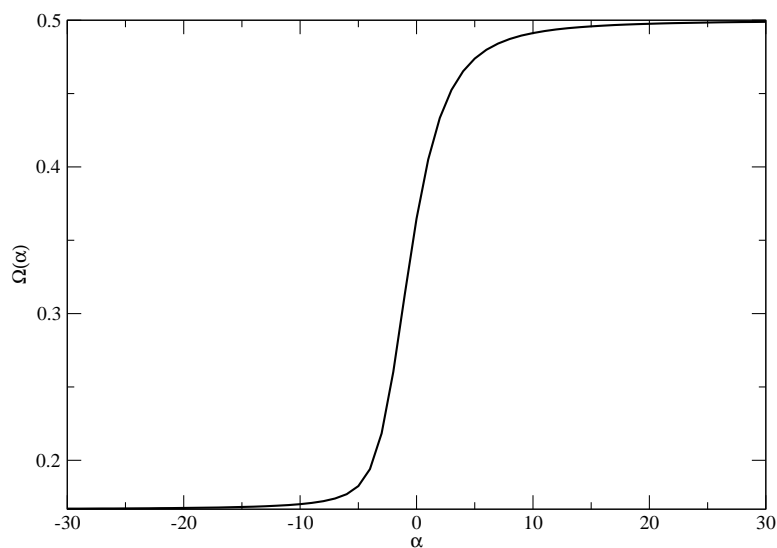


Figure 2: Plot of $\Omega(\alpha)$ as a function of α showing the behavior of the scaled function.

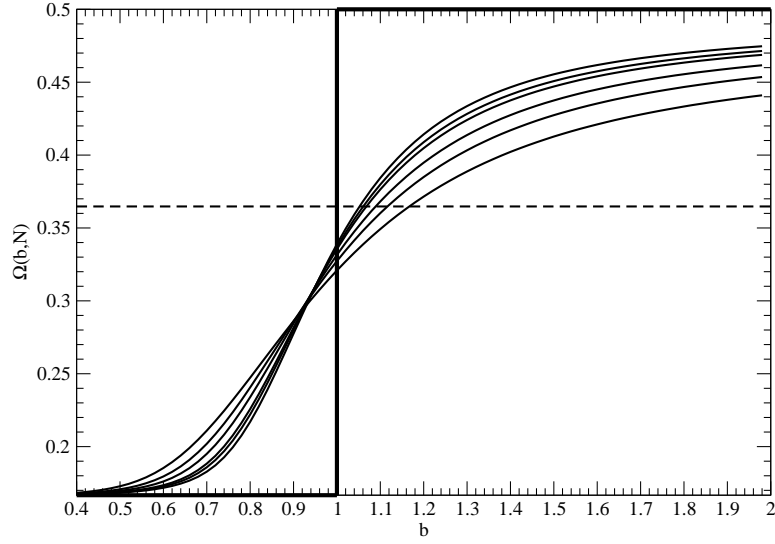


Figure 3: Plot of $\Omega(b, N)$ as a function of b for several N . $N = 17, 23, 29, 37, 41, 47$ are the values in the plot and they gradually approach the critical behavior at $N = \infty$. The dashed line is the value of Ω at the critical point obtained using the double scaling limit.

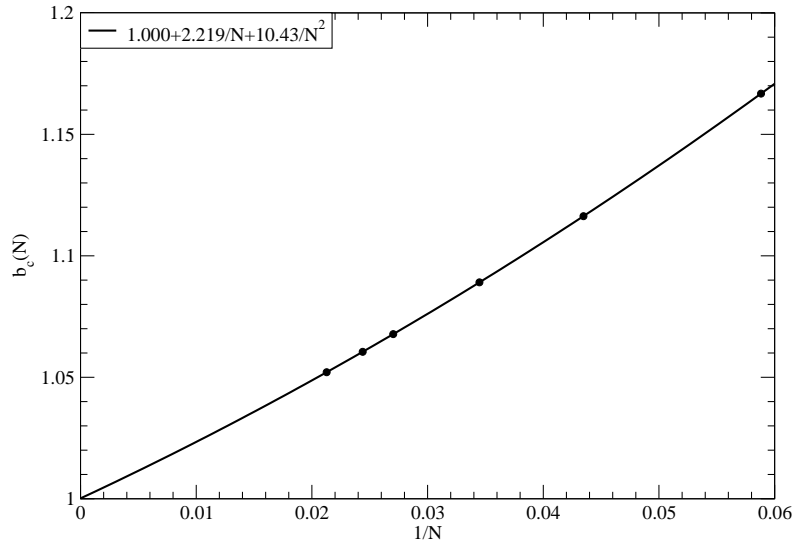


Figure 4: Plot of $b_c(N)$ as a function of $\frac{1}{N}$.

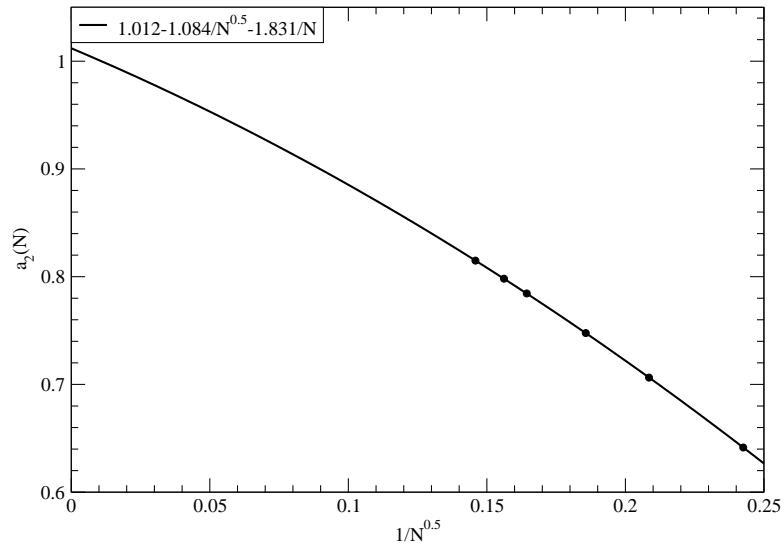


Figure 5: Plot of $a_2(N)$ as a function of $\frac{1}{\sqrt{N}}$.

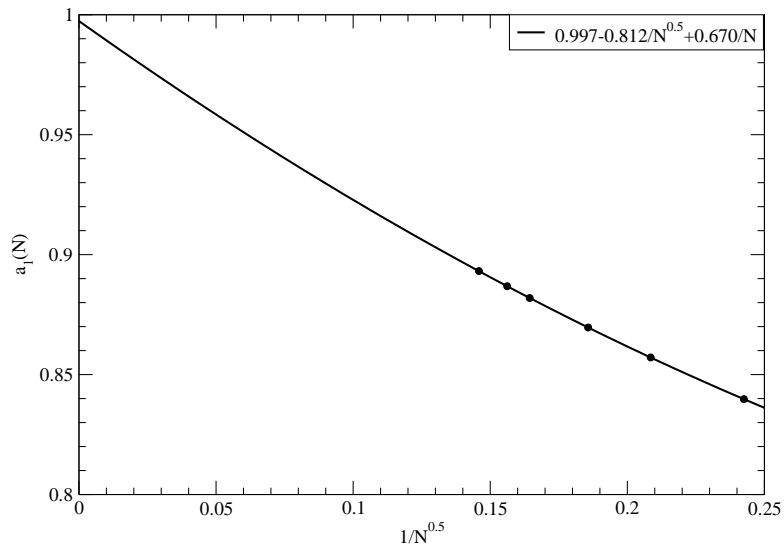


Figure 6: Plot of $a_1(N)$ as a function of $\frac{1}{\sqrt{N}}$.

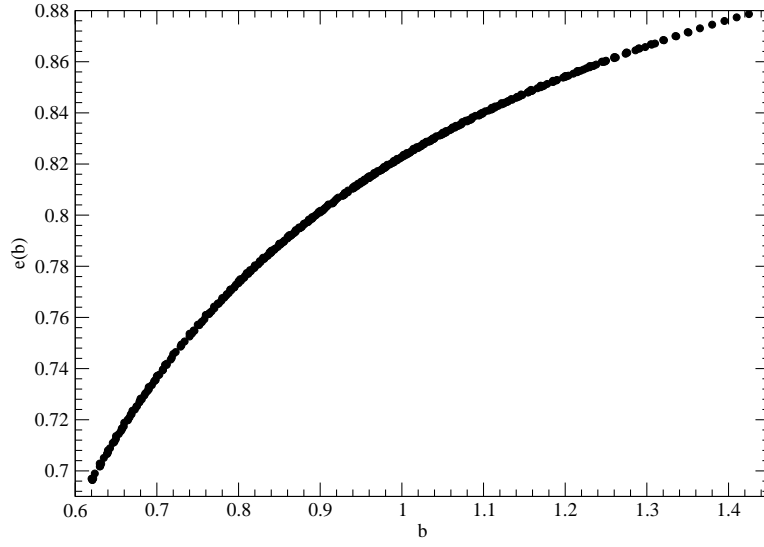


Figure 7: Plot of the average plaquette, $e(b)$, as a function of b .

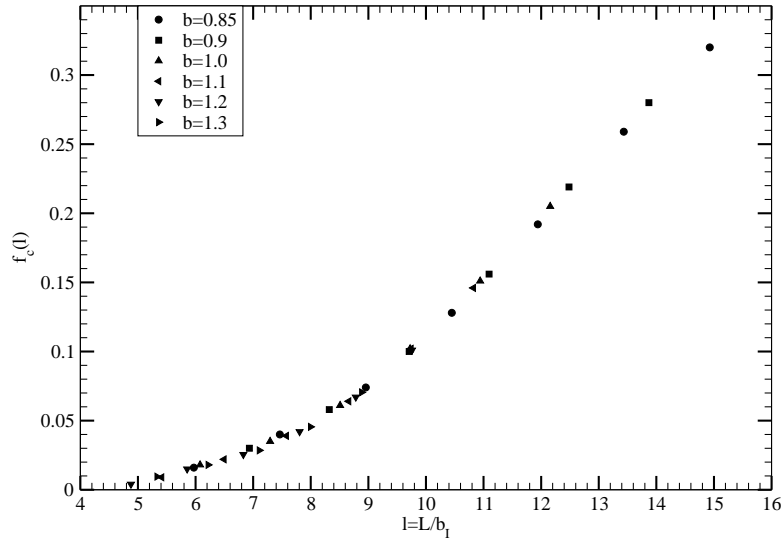


Figure 8: Plot of the critical value of the smearing parameter as a function of the size of the loop.

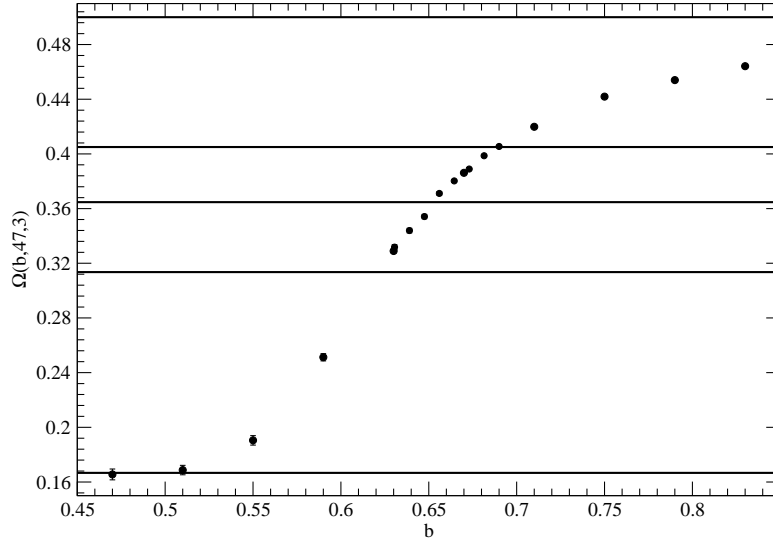


Figure 9: Plot of the $\Omega(b, N, L)$ as a function of b for $N = 47$ and $L = 3$ on a 4^3 lattice.

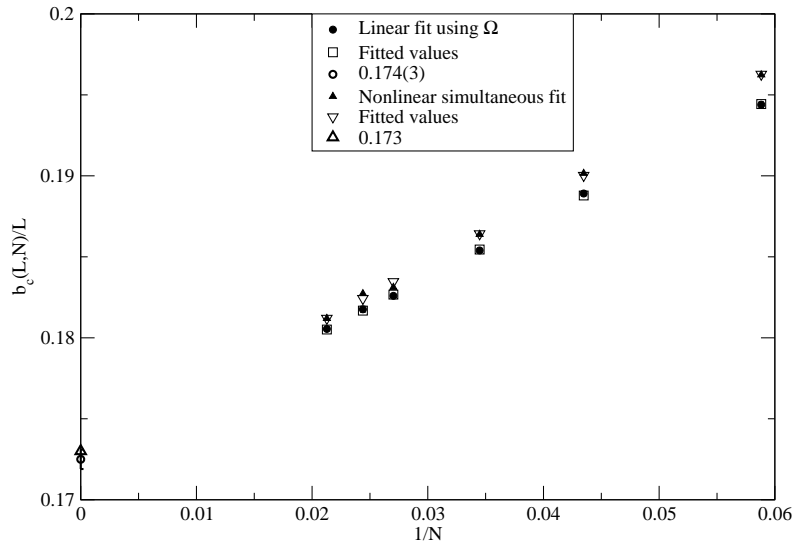


Figure 10: Plot of the $\frac{b_c(L, N)}{L}$ as a function of $1/N$ for $L = 6$ on a 8^3 lattice.

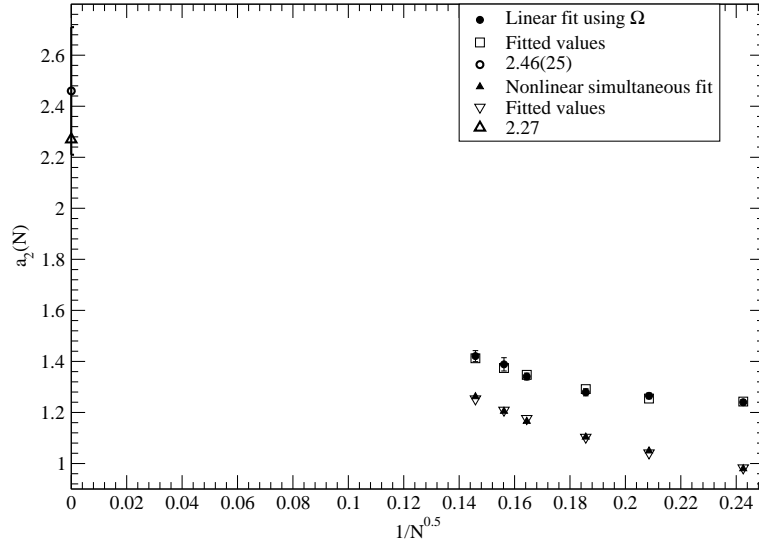


Figure 11: Plot of the $a_2(L, N)$ as a function of $1/\sqrt{N}$ for $L = 6$ on a 8^3 lattice.

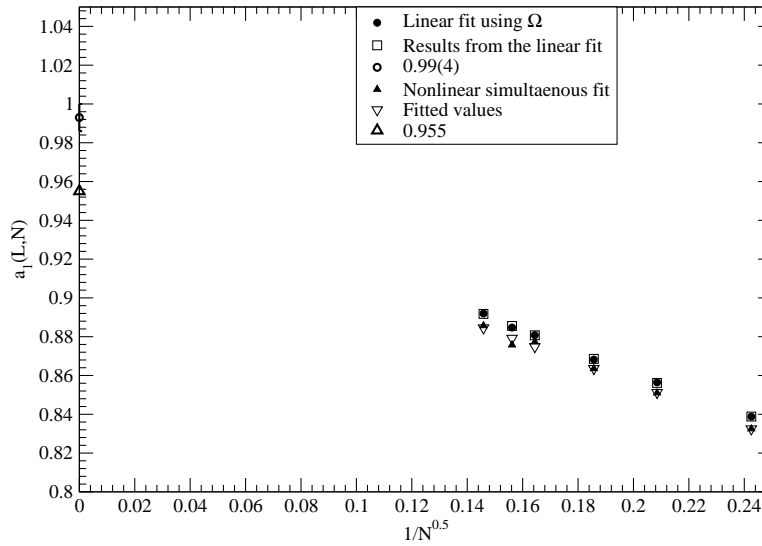


Figure 12: Plot of the $a_1(L, N)$ as a function of $1/\sqrt{N}$ for $L = 6$ on a 8^3 lattice.

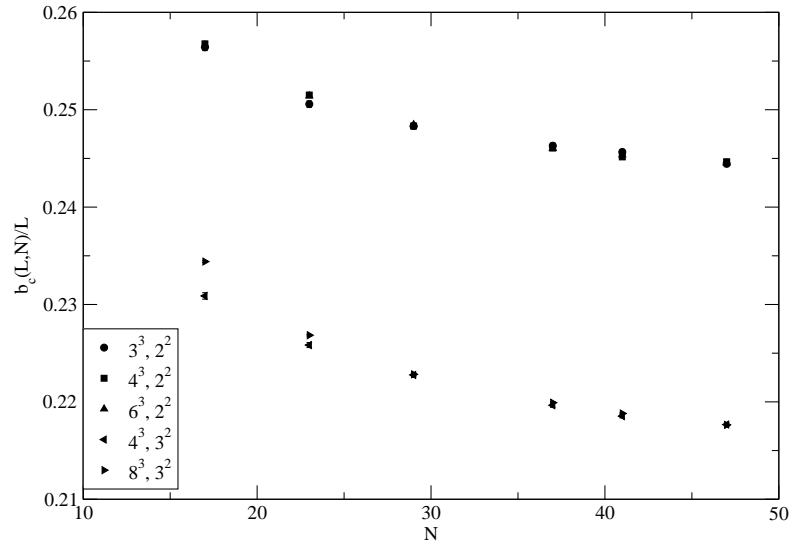


Figure 13: Plot of the $\frac{b_c(L, N)}{L}$ as a function of N for different lattices sizes and $L = 2, 3$.

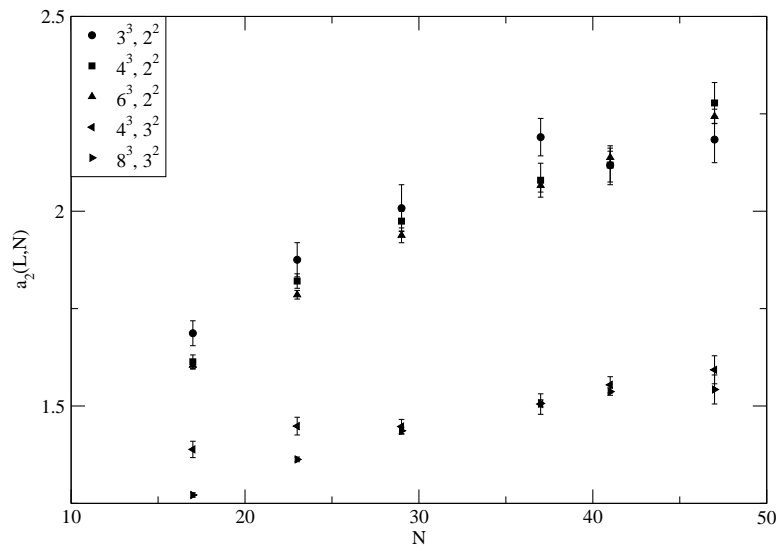


Figure 14: Plot of the $a_2(L, N)$ as a function of N for different lattices sizes and $L = 2, 3$.

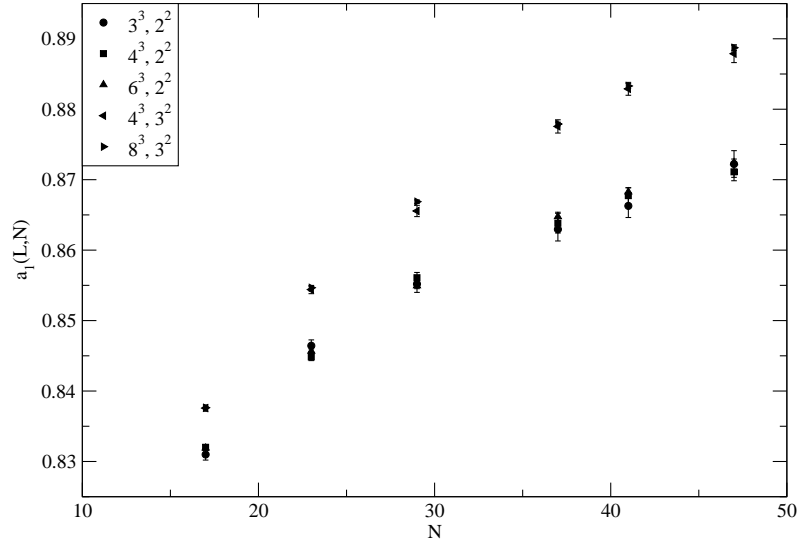


Figure 15: Plot of the $a_1(L, N)$ as a function of N for different lattices sizes and $L = 2, 3$.

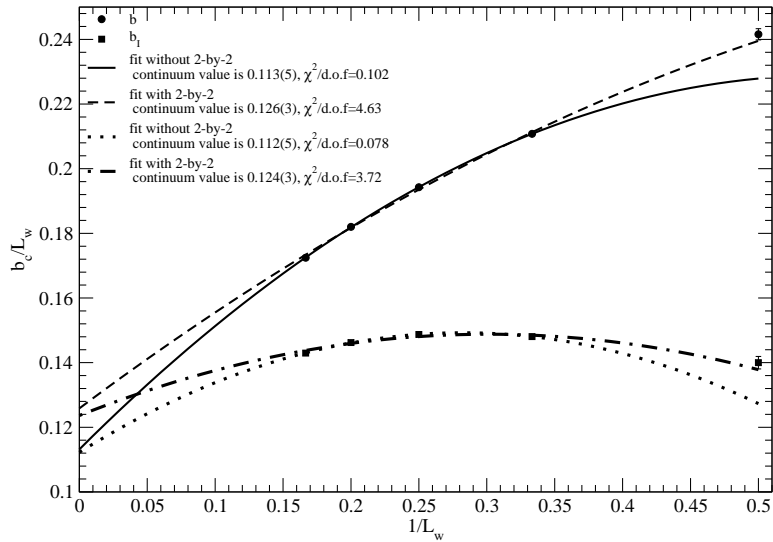


Figure 16: Plot of the $\frac{b_c(L, \infty)}{L}$ as a function of $1/L$.

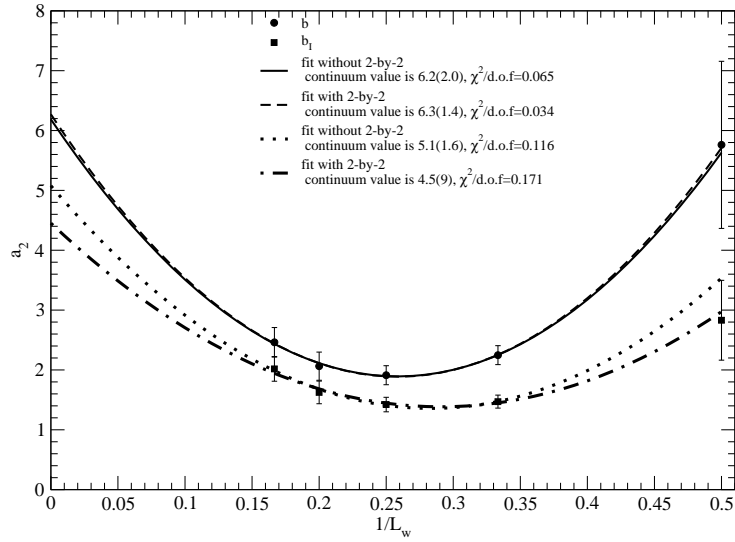


Figure 17: Plot of $a_2(L, \infty)$ as a function of $1/L$.

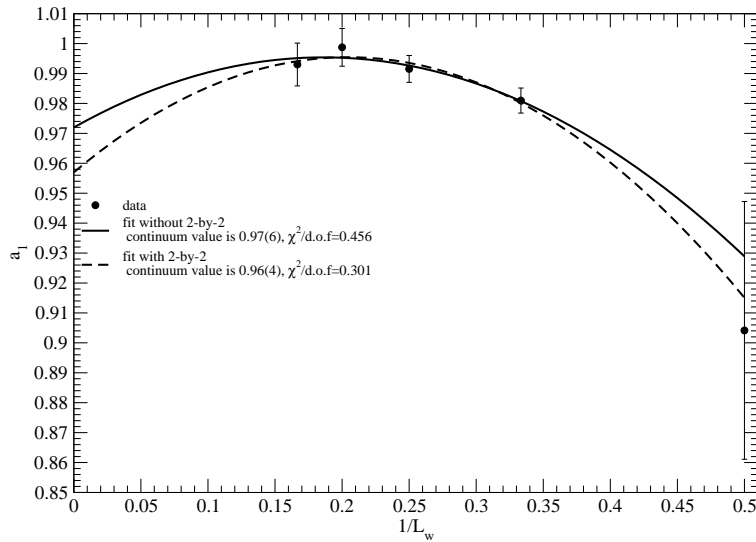


Figure 18: Plot of $a_1(L, \infty)$ as a function of $1/L$.